Genetic analysis

Genomic DNAs were prepared from ethylene diamine tetra acetic acid (EDTA)-treated whole blood samples using a QIAamp DNA Blood kit (Qiagen, Hilden, Germany). All exons and their flanking intronic splice sites of genes encoding major subunits of sodium channels (*SCN1A*, *SCN2A*, *SCN1B* and *SCN2B*) and $GABA_A$ receptors (*GABRA1*, *GABRB2* and *GABRG2*) were screened for abnormalities using a direct sequencing method with an automatic sequencer as described previously (Fukuma et al., 2004; Hirose et al., 1999, 2000; Ishii et al., 2009). Details of the PCR conditions and the primers used are available upon request. Reference sequences of mRNA were based on information available from RefSeq (accession numbers): Human *SCN1A*, NM006920; Human *SCN2A*, NM021007; Human *SCN1B*, NM001037; Human *SCN2B*, NM004588; Human *GABRA1*, NM000806; Human *GABRB2*, NM021911; Human *GABRG2*, NM19890; and Rat *Gabrg2*, NM183327.

Recombinant constructs

Full-length Rattus $\alpha 1$, $\beta 2$, and $\gamma 2$ subunit cDNAs containing either the *myc* epitope tags (between amino acids 4 and 5 of the mature polypeptide) have been described previously (Connolly et al., 1996) and shown to be functionally silent with respect to receptor pharmacology and physiology. The cDNAs were subcloned into pcDNA3.1 (Invitrogen, Carlsbad, CA) and pIRES-EGFP (Clontech, Mountain View, CA). The mutant expression construct $\gamma 2$ (p.Q40X) was generated in each construct using the QuickChange Site-Directed mutagenesis kit (Stratagene, La Jolla, CA). Clones were validated by direct double-strand DNA sequencing on an ABI3100 sequencer using DyePrimer chemistry (Applied Biosystems, Foster City, CA).

Tissue culture and transfection

HEK293T cells were grown in Dulbecco's modified Eagle medium (DMEM; Bio-Whitaker, Walkersville, MD) supplemented with 10% fetal bovine serum and transfected using FuGene 6 transfection reagents (Roche Applied Science, Indianapolis, IN). Cells were incubated for 24 h at 37 °C in a humidified incubator containing 5% CO_2.

Electrophysiological studies

cDNA constructs for rat $GABA_A$ receptor subunits were transferred to the eukaryotic expression vector, pcDNA3 (Invitrogen). cDNA constructs for CD8 in the expression vector piH3 were provided by B. Seed (Massachusetts General Hospital, MA). HEK293 cells (Japanese Collection of Research Bioresources, Japan) were cultured in DMEM (Gibco, Tokyo, Japan) supplemented with 7% fetal bovine serum (Gibco), 7% horse serum (Sigma, St. Louis, MO), L-glutamine (Gibco, USA), and gentamicin (Boehringer Mannheim, Mannheim, Germany), in a humidified atmosphere containing 5% CO_2 and 95% air, at 37 °C. The cells were passaged twice a week and used at 8 ± 16 passages (mean $\pm$ SD). The cells were plated at 1×10^5 cells/35-mm culture dish containing poly-l-lysine (Sigma) and collagen (Vitrogen100, USA)-coated coverslips, the day before transfection. HEK293 cells were transfected with cDNAs (total 1.0 g for all subtypes and 0.1 g of CD8) using Lipofectamine (Gibco), and the conventional whole-cell patch clamp recordings were obtained at 36–72 h after transfection. Cells highly expressing the $GABA_A$ receptor channels were identified under a microscope using the bead-labeling technique (Jurman et al., 1994), with beads covalently coupled antibody to CD8 (Dynabeads, Invitrogen, Carlsbad, CA). The pipette solution contained (in mM): CsCl 140, $MgCl_2$ 2, EGTA 5, and HEPES 10 (pH 7.2 with CsOH). The pipette resistance was approximately 5 MΩ. The series resistance (2–8 MΩ) and the cell capacitance (12–80 pF) were compensated up to 80%. In all cases, data were obtained from isolated single cells. All currents were filtered at 1 kHz and measured with an Axopatch 200 A amplifier (Axon Instruments, Palo Alto, CA). Data obtained were then sampled at 5 kHz and stored using pClamp ver. 9 (Axon Instruments). The external solution contained (in mM): NaCl 150, KCl 5.0, $MgCl_2$ 2.0, $CaCl_2$ 2.0, D-glucose 10, and HEPES 10 (pH 7.4 with NaOH). The bath solution was perfused at 1 ± 2 ml/min from a separate perfusion line and removed from the bath with an aspirator. Each drug was applied through polyethylene Y-tube (equilibration time <20 ms) by gravity feed (Ueno et al., 1997). GABA was applied at an interval of 4 min to avoid running down of the current responses. All experiments were performed at room temperature (20–25 °C).

Immunohistochemistry

Patient brain obtained at autopsy was fixed in formalin and embedded in paraffin. Control brain specimens (temporal lobe, basal ganglia, and thalamus) were obtained from a 3-year-old boy who died from acute lymphocytic leukemia. Sections of formalin-fixed and paraffin-embedded tissues were cut at 4 μm thickness and immunohistochemically stained using the streptavidin–biotin method with antibodies against $GABA_A$ receptor $\alpha 1$ and $\beta 2$ subunits. The sections were deparaffinized in xylene and then rehydrated in ethanol. Endogenous peroxidase activity was blocked with 3% H_2O_2 in methanol and then antigen retrieval was achieved using microwave irradiation. After cooling to room temperature, the sections were washed thoroughly in Tris-buffered saline (TBS), and then incubated overnight at 4 °C with anti-$GABA_A$ receptor $\alpha 1$ antibody (dilution 1:100, Upstate Biotechnology, New York, NY) and overnight at 4 °C with $GABA_A$ receptor $\gamma 2$ antibody (dilution, 1:200, Alpha Diagnostic International Inc., TX). After three washes in TBS, biotinylated secondary antibodies and peroxidase-conjugated streptavidin [Simplestain MAX-PO (MULTI), Nichirei, Tokyo] were applied to the sections (the former at 4 °C overnight and the latter at room temperature for >2 h). After three washes in TBS, the immunoproducts were visualized using diaminobenzidine (Nichirei), and the sections counterstained with hematoxylin.

Microinjection

HEK293T cells were cultured on a coverslip, and microinjection was performed using a semi-automated microinjection

system (InjectMan; Eppendorf, Hamburg, Germany). For nuclear injections, plasmids were used at 100 mg/ml.

Immunostaining of HEK293T cells

HEK293T cells were fixed with 4% paraformaldehyde in phosphate buffered saline (PBS) at room temperature for 7 min. Cells were washed and permeabilized with 0.1% Triton X-100 in PBS at room temperature for 5 min, and finally rinsed three times with 0.1% bovine serum albumin (BSA) in PBS. Fixed cells were incubated with the primary antibody diluted in PBS with 0.1% BSA at appropriate concentrations for 40 min at 37 °C. The antibodies used included anti-myc 10 mg/ml and rabbit monoclonal PDI (dilution 1:1000; Affinity Bioreagents, Golden, CO). This incubation was followed by three washes with 0.1% BSA in PBS and another incubation with Alexa Fluor goat anti-mouse or anti-rabbit antibody (dilution 1:1000; Molecular Probes, Eugene, OR) for 40 min at 37 °C. ProLong Gold Antifade Kit (Molecular Probes) was used to mount sections onto glass slides according to the instructions supplied by the manufacturer. Fluorescently labeled cells were visualized by standard fluorescence microscopy and confocal microscopy (model 510 META, Carl Zeiss, Jena, Germany).

Quantification of the localization of $GABA_A$ receptor

The quantification procedure was comprised of cDNA microinjection, staining, and cell counting, and this procedure was independently replicated three times for each $GABA_A$ receptor: WT $\alpha 1 myc \beta 2 \gamma 2$ (WT receptor), heterozygous $\alpha 1 myc \beta 2 \gamma 2 \gamma 2$ (Q40X, heterozygous receptor), and homozygous $\alpha 1 myc \beta 2 \gamma 2$ (Q40X, homozygous receptor). HEK293T cells were fixed at 4 or 18 h (short and long incubation, respectively) after the microinjection of cDNAs of the WT, heterozygous, or homozygous receptors, and labeled with secondary antibodies Alexa 488 (green) and Alexa 594 (red) (Molecular Probes) anti-*myc* and anti-PDI, respectively. Then, cells were mounted on glass slides with DAPI. The number of cells expressing the $\alpha 1$ subunit was quantified by counting nuclei stained with DAPI in cells that satisfied the conditions for *myc* (green) to match the cell morphology in the bright field. Some cells burst during and after the microinjection process; all remaining cells that were alive and stained with *myc*-tag were counted. For the WT receptor, the total number of cells counted was 66 (15, 21, and 30 in each of the three independent replications) at 4-h incubation, and 81 (40, 23, and 18) at 18-h incubation. For the heterozygous receptor, total number of cells counted was 47 (13, 22, and 12 in each of the three independent replications) at 4-h incubation, and 54 (19, 16, and 29) at 18-h incubation. For the homozygous receptor, the total number of cells counted was 114 (62, 15, and 37 in each of the three independent replications) at 4 h, and 137 (28, 47, and 62) at 18-h incubation. Colocalization with ER was determined based on overlapping *myc* and PDI staining. The colocalization with the plasma membrane was determined based on *myc* staining and the cell shape observed under the bright field. Cells that showed *myc* staining both on the membrane and in the ER were allocated to the membrane or ER colocalization based on the predominant staining location. Predominant location was based on the percentage of receptor distribution between the cell membrane and ER, and was determined relative to the total number of cells in both cases.

Culture of hippocampal neurons and transfection

Mouse hippocampal neurons were cultured as described previously with slight modifications (Brewer et al., 1993). Briefly, hippocampi from P1 pups were extirpated and placed into ice-cold Leibovitz L-15 (L-15) solution supplemented with 0.2 mg/ml BSA. These tissues were then digested with 0.4% DNase I and 0.25% trypsin in L-15/BSA for 15 min at 37 °C. The digested samples were then transferred to culture media (Neurobasal-A) supplemented with B-27, 5 μg/ml insulin, 5 μg/ml transferrin, and 5 ng/ml sodium selenite, followed by trituration by passing them through a Pasteur pipette until the disappearance of visible tissue fragments. We calculated the number of cells in the cell suspension and diluted it by adding an adequate amount of culture media. The cells were plated onto 22-mm × 22-mm coverslips precoated with L-polylysine and incubated in culture media at a density of ca. 250 cells/mm^2. Six days after plating, the cells were transfected using Lipofectamine LTX with either WT cDNA or the Q40X mutant construct of $GABA_A$ receptor γ subunit constructed in pEGFP-C1 (Clontech). The culture medium was changed on the next day and the cells were maintained for two more days.

Immunocytochemistry of cultured hippocampal neurons

For immunocytochemistry, the cultured neurons were briefly rinsed with prewarmed PBS twice, followed by fixation in 3.7% formaldehyde for 30 min at 37 °C. After fixation, the cells were rinsed 3 times with PBS, and then treated with 0.25% Triton X-100 for 10 min at room temperature (RT) to permeabilize the cell membranes. The cells were then treated with 2% skim milk in PBS for 30 min to attenuate non-specific binding. Subsequently, the cells were incubated overnight at 4 °C with primary antibodies, followed by three washes in PBS and blocking with 2% skim milk for 30 min at RT. The cells were then incubated with fluorophore-conjugated secondary antibody (Molecular Probes) for 2 h at RT. After thorough washing with PBS, the cells were stained with DAPI to visualize nuclei, and viewed under the confocal fluorescence microscope (FV-1000, Olympus, Tokyo).

Primary antibodies used to stain neurons

The following primary antibodies were used to detect and specify the localization of GABA receptors: anti-$GABA_A$ receptor $\beta 2$, 3-subunit antibody (Cat# MAB341, Millipore, Bedford, MA), anti-$GABA_A$ receptor antibody α-subunit (Cat# 06-868, Upstate Biotechnology), anti-$GABA_A$ receptor antibody $\gamma 2$-subunit (Cat# NB300-151, Novus, USA), anti-myc antibody (Clone 9E10, Sigma), anti-calnexin antibody (Cat# 610523, BD Transduction Laboratories, San Jose,

CA), anti-PDI antibody (Cat# SPA-890, StressGen Biotechnology, Victoria, BC, Canada), and anti-GFP antibody (Cat# AB16901, Millipore).

Statistical analysis

Data were expressed as mean ± SD. Differences in the distribution of $GABA_A$ receptors among genotypes were analyzed by analysis of variance with Scheffe's multiple comparison using GLM (general linear model). Statistical significance of electrophysiological data was determined by one-way ANOVA, followed by Dunnett's method as post hoc test. All statistical analyses were performed using the Statistical Analysis System software (version 9.2, SAS Institute Inc., Cary, NC). A *P* value of <0.05 denoted the presence of significant statistical difference.

Results

Pedigree of twins with Dravet syndrome and a *GABRG2* mutation (p.Q40X)

Genetic analyses were performed for several Dravet syndrome candidate genes. The selected genes are known to encode components of neuronal sodium channels (*SCN1A, 2A, 1B, 2B*) or $GABA_A$ receptors (*GABRA1, B2, G2*) and contain mutations associated with both Dravet syndrome and GEFS+. A single *GABRG2* mutation (c.118C>T, based on a human *GABRG2* cDNA: RefSeq NM_198904) was identified in dizygotic twin girls with Dravet syndrome and in their apparently healthy father, but not in their mother who experienced seizures during childhood (Fig. 1A). No other mutation was detected within the examined regions of *GABRG2* or the other genes. The mutation was heterozygous and not found in other family members, including the mother with history of epilepsy and 182 healthy Japanese volunteers (Fig. 1B). The mutation was deduced to be associated with premature termination codons (PTCs) at position 40 of the GABRG2 molecule (p.Q40X) (Fig. 1D). The resultant mutated γ2 subunit was truncated at the N terminus after a very short amino acid sequence (Fig. 1C).

Electrophysiological properties of $GABA_A$ receptor bearing p.Q40X in γ2 subunit

To gain insight into the functional consequences of the p.Q40X mutation in the γ2 subunit, we analyzed GABA-mediated currents in HEK293 cells expressing α1β2, wild type (WT) α1β2γ2, heterozygous α1β2γ2γ2 (Q40X), or homozygous α1β2γ2 (Q40X) $GABA_A$ receptors (Fig. 2). HEK293 cells expressing WT subunits produced a robust inward current in response to GABA. $GABA_A$ receptors consisting of α1 and β2 subunits only also produced an inward current in response to GABA. However, peak currents and current density were decreased compared to those of $GABA_A$ receptors consisting of WT α1β2γ2. The inward currents and current density of homozygous α1β2γ2 (Q40X) were intermediate between WT α1β2γ2 and heterozygous α1β2γ2γ2 (Q40X) $GABA_A$ receptors. This result suggested that mutant γ2 (Q40X) had haploinsufficiency effect. Interestingly, peak currents and current density obtained from $GABA_A$ receptors were decreased when cDNAs of the mutant γ2 (Q40X) were transfected with those of other components of $GABA_A$ receptor, α1 and β2 subunits. This result suggests that the effect of the mutant γ2 (Q40X) subunit on the $GABA_A$ receptor function was loss of function or dominant-negative suppression when current densities were compared.

Immunohistochemistry of patient brain

Immunohistochemical assay of the patient and control brain specimens using anti-α1 subunit and anti-γ2 subunit antibody was performed to determine the change in $GABA_A$ receptor subunit (Fig. 3). In the patient brain specimens immunostained for γ2 subunits, granules were observed in neuronal soma and neuropils. The same granules were also observed in neuronal soma and neuropils stained with antibody against α1 subunits of $GABA_A$ receptor. These findings suggest that $GABA_A$ receptor harboring the mutant γ2 (Q40X) subunit form aggregates in brain cells. It has been reported that deficient $GABA_A$ receptors precipitate in the ER (Harkin et al., 2002; Kang and Macdonald, 2004).

Localization of α1 subunits in HEK293T

To map the intracellular localization of the mutant molecules, HEK293T cells, were transiently microinjected with pcDNA-3.1 vectors bearing either WT $\alpha1^{myc}\beta2\gamma2$ or homozygous $\alpha1^{myc}\beta2\gamma2$ (Q40X) cDNA. These cells were subsequently immunostained for *myc* to visualize the channel proteins. In HEK293T cells, the distribution of the mutant subunits [homozygous $\alpha1^{myc}\beta2\gamma2$ (Q40X)] associated with Dravet syndrome differed from that of WT protein. The α1 subunit was expressed on the cell surface and in the ER, as shown by co-staining for the ER marker protein disulfide isomerase (PDI) at 6 h after microinjection (data not shown). The combinations of receptors produced from α1 and β2 subunits are capable of exiting the ER and accessing the cell surface. Therefore, the $GABA_A$ receptors expressed on the cell surface are likely to be those subunits that could elude the trafficking disruption due to the mutant γ2 (Q40X) molecules.

We next considered the role of γ2 subunits in the cells. These subunits are known to be important in conferring benzodiazepine sensitivity on $GABA_A$ receptors and in controlling the synaptic targeting of these receptors (Essrich et al., 1998; Gunther et al., 1995). Furthermore, the γ2 subunits participate in the translocation of $GABA_A$ receptor to the cell membrane (Keller et al., 2004; Kittler et al., 2002; Moss and Smart, 2001; Sarto et al., 2002), and to act with $GABA_A$ receptor-associated protein (GABARAP) in other intercellular transportation of the GABA receptor (Kanematsu et al., 2002; Kittler et al., 2001, 2002; Kneussel, 2002; Wang et al., 1999). The above studies suggested that the *GABRG2* early truncation mutation (p.Q40X) could induce a delay in $GABA_A$ receptor trafficking to the cell surface.

To investigate the effect of the mutated γ2, we studied the time course of trafficking of $GABA_A$ receptor harboring the mutated γ2 after microinjection of the relevant cDNAs and the effect of dose of the mutated γ2

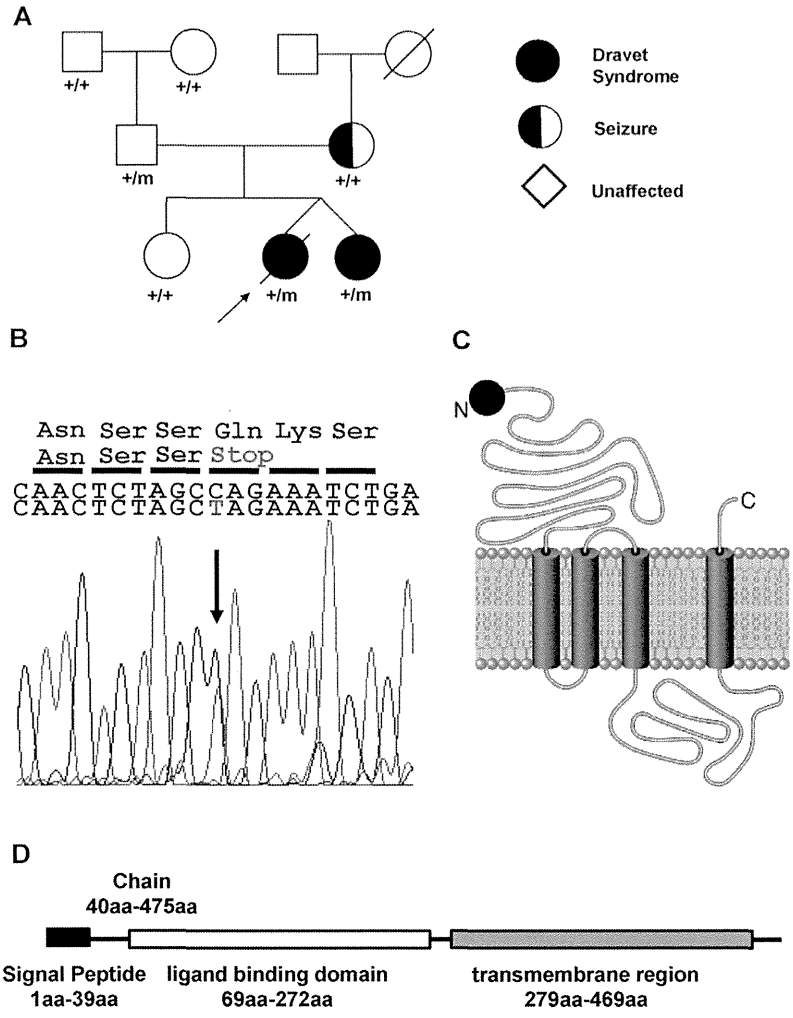

Figure 1 (A) Pedigree of the patient with Dravet syndrome and mutation analysis. *Arrow*: the proband, *squares*: males, *circles*: females. +: wild type allele, m: allele found to have a p.Q40X mutation. The mutation c.118C>T: p.Q40X in *GABRG2*, which was detected in dizygotic twin girls with Dravet syndrome and their apparently healthy father, but not in their mother who experienced seizures in childhood. The father's mutation was *de novo*. (B) Nucleotide sequence of the relevant region of *GABRG2* in the patient. Genomic DNA from the patient was amplified for exon 2 of *GABRG2* by PCR. The nucleotide sequences of the products were determined sequencing, in the 5′—3′ direction. *Arrow:* nucleotide 118, where three nucleotides were changed by the mutation. (C) Schematic representation of the GABRG2 protein product showing the position of the p.Q40X mutation. (D) Mutational position in the GABRG2 protein (arrow). *Solid square*: Signal peptide located from 1 to 39 amino acid, *open square*: Ligand binding domain, *gray square*: Transmembrane domain. The mutation p.Q40X is located directly below the signal peptide, resulting in a truncated GABRG2 protein with complete loss of the ligand binding domain and the transmembrane domain.

(i.e., heterozygous or homozygous of the mutated γ2). We carried out a short (4 h) and long (18 h) incubations of WT $\alpha1^{myc}\beta2\gamma2$-, heterozygous $\alpha1^{myc}\beta2\gamma2\gamma2$ (Q40X)-, and homozygous $\alpha1^{myc}\beta2\gamma2$ (Q40X)-injected cells. Microscopic analysis of these cells demonstrated the majority of the $\alpha1^{myc}$ subunit for WT, heterozygous, and homozygous receptors colocalized with PDI in the case of shorter incubation (4 h) after microinjection (Fig. 4A), and only WT cells had identifiable $\alpha1^{myc}$ subunit colocalized with the membrane. In contrast, the majority of the $\alpha1^{myc}$ subunit for heterozygous and homozygous receptors was retained in the ER even in the case of longer incubations (18 h) after microinjection (Fig. 4B). Quantification of the localization of the $\alpha1^{myc}$ subunit was done by the manual counting of cells showing myc staining colocalized with the membrane or ER, and each quantification procedure was replicated three times. For the WT receptor, 66 cells (15, 21, and 30 cells in each of the three independent replications) were counted in the short incubation condition (i.e., 4 h), and 81 (40, 23, and 18) cells in the long incubation condition (i.e., 18 h); all these cells expressed the $\alpha1^{myc}$ subunit. In the short incubation condition, the $\alpha1^{myc}$ subunits were found predominantly on the membrane in 15 of the cells (4, 7, and 4 in each of the three independent replications), whereas the $\alpha1^{myc}$ subunits were found predominantly in the ER of the 51 remaining cells (11, 14, and 26). In contrast, in the long incubation condition, the $\alpha1^{myc}$ subunits were found predominantly on the membrane in 61 of the cells (22, 21, and 18 in each of the three independent replications), whereas the $\alpha1^{myc}$ subunits were

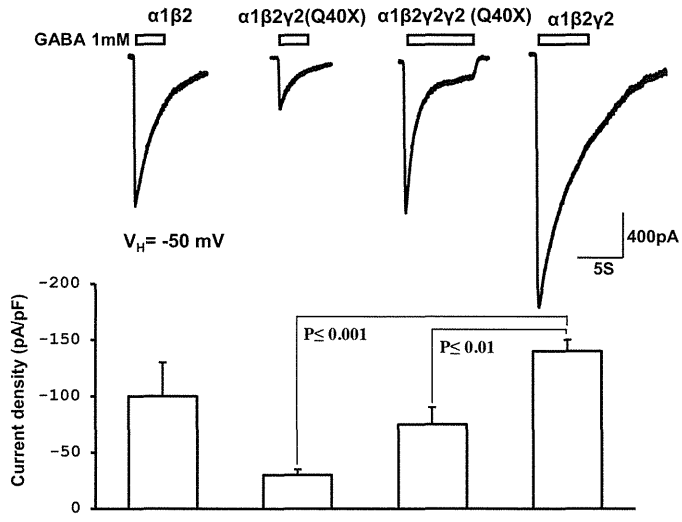

Figure 2 Electrophysiological properties of $GABA_A$ receptor γ2 subunit bearing p.Q40X mutation. Electrophysiological studies were performed to evaluate the function of $GABA_A$ receptors reconstituted with α1, β2, and γ2 subunits in HEK cells. Additional transfection of mutated γ2 (Q40X) suppressed GABA-induced current amplitudes for the $GABA_A$ receptors. Data are mean ± SD of 5 (α1β2), 6 [α1β2γ2 (Q40X)], 6 [α1β2γ2γ2 (Q40X)] and 8 (α1β2γ2) samples.

observed predominantly in the ER in the 20 remaining cells (18, 2, and 0).

For the heterozygous receptor, 47 cells (13, 22, and 12 in each of three independent replications) were counted in the short incubation condition, and 64 cells (19, 16, and 29) in the long incubation condition; all cells expressed the $\alpha1^{myc}$ subunit. In the short incubation condition, the $\alpha1^{myc}$ subunits were found predominantly on the membrane in 3 cells (2, 1, and 0 in each of the three replications), whereas the $\alpha1^{myc}$ subunits were found predominantly in the ER in 44 cells (11, 21, and 12). In the long incubation condition, the $\alpha1^{myc}$ subunits were found predominantly on the membrane in 34 cells (9, 9, and 16 in each of the three replications), whereas the $\alpha1^{myc}$ subunits were observed dominantly in the ER in 30 cells (10, 7, and 13).

For the homozygous receptor, 114 cells (62, 15, and 37 in each of the three replications) were counted in the short incubation, and 137 cells (28, 47, and 62) in the long incubation; all cells expressed the $\alpha1^{myc}$ subunit. In the short incubation, the $\alpha1^{myc}$ subunits were found predominantly

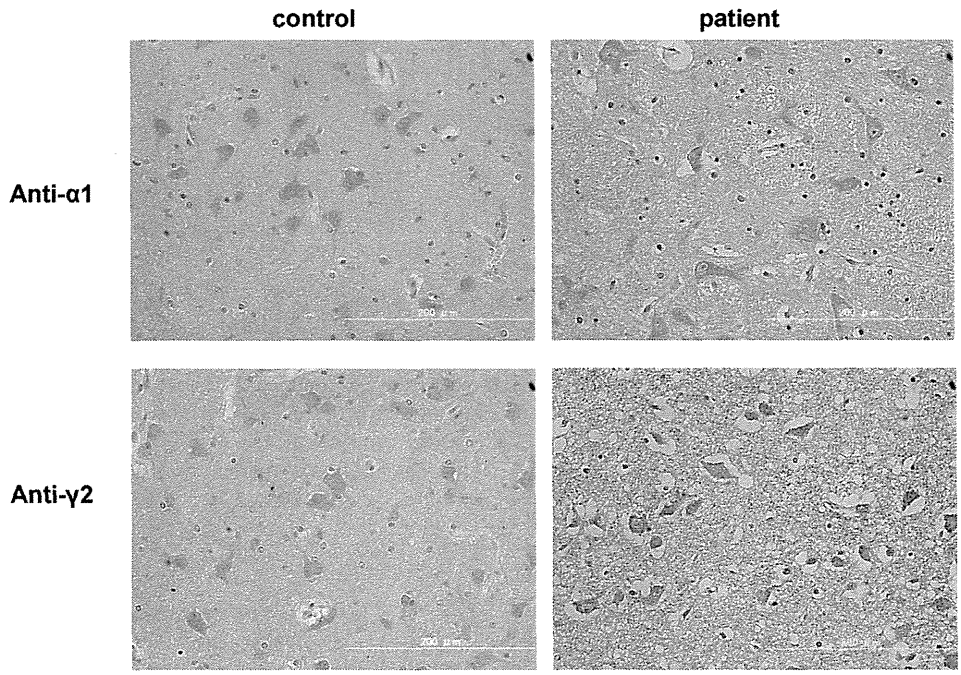

Figure 3 Immunohistochemistry of brain tissues. Immunostaining of brain tissue from one of the twins with antibodies against α1 and γ2 subunits revealed partial loss of reactivity and granules in the somas of some neurons and neuropils. Magnification, 250×.

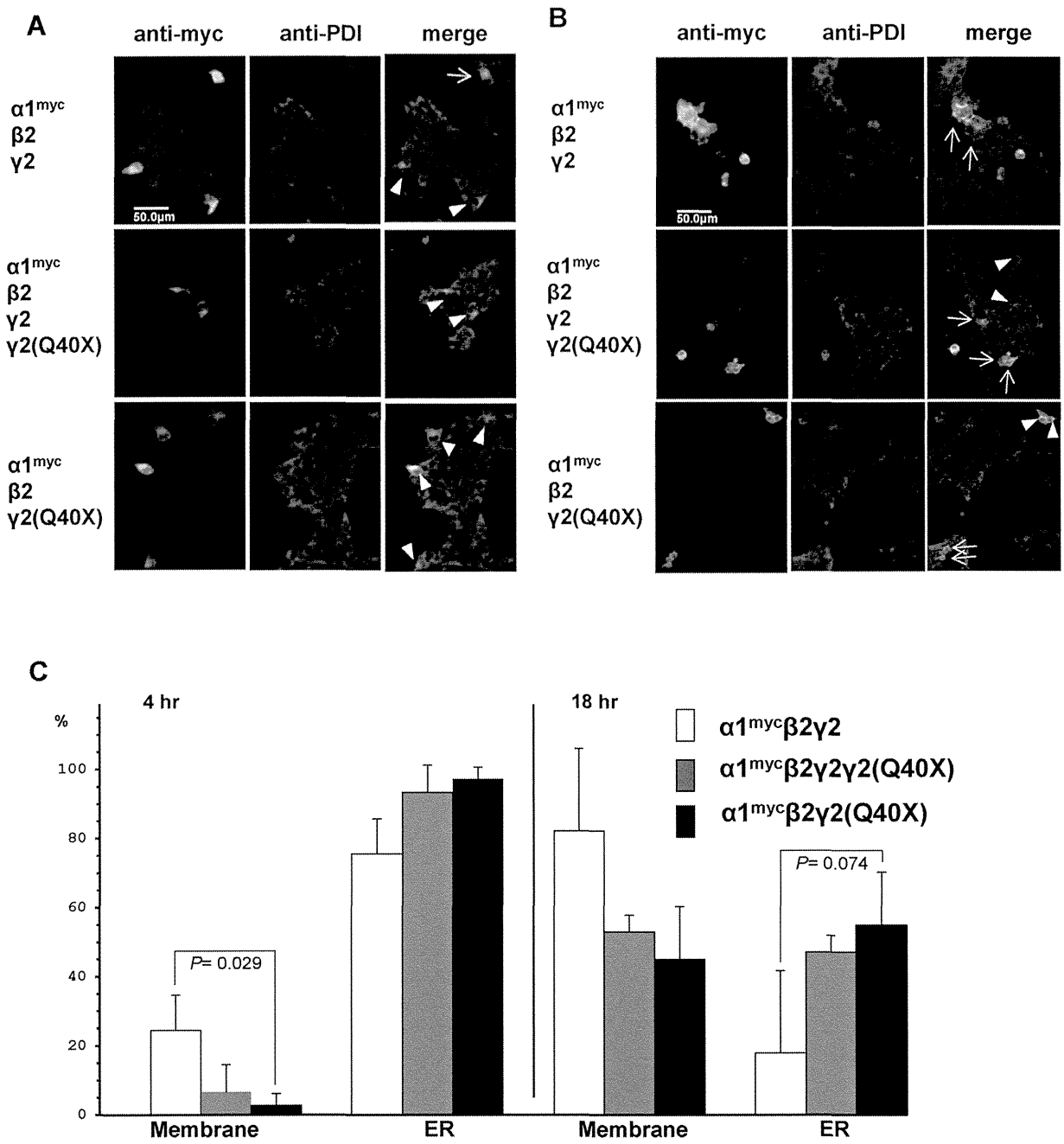

Figure 4 Localization of α1 subunits in HEK293T cells after short (4 h) and long (18 h) incubation periods. HEK293T cells were microinjected with wild type $\alpha1^{myc}\beta2\gamma2$, heterozygous $\alpha1^{myc}\beta2\gamma2\gamma2$ (p.Q40X), and homozygous $\alpha1^{myc}\beta2\gamma2$ (p.Q40X). After 4 h or 18 h harvest, cells were fixed and stained with antibodies for the myc-tag (green) and PDI (red). (A) The majority of wild type, heterozygous, and homozygous proteins colocalized with the ER (triangle). However, only some of the wild type also colocalized with the plasma membrane (arrow). (B) Approximately half of the heterozygously and homozygously expressed transcripts remained in the ER (triangle), while the majority of wild type protein colocalized with the membrane (arrow). (C) Quantitative analysis of the fractions of total wild type, heterozygous, and homozygous $GABA_A$ receptors that colocalized to the membrane and ER. Data are mean ± SD of the fractions of colocalization elucidated from three independent replications.

on the membrane in only 2 cells (1, 1, and 0 in each of the three replications), whereas the $\alpha1^{myc}$ subunits were found predominantly in the ER in 112 cells (61, 14, and 37). Even in the long incubation condition, the $\alpha1^{myc}$ subunits were found predominantly on the membrane in only 59 cells (13, 28, and 18 in each of the three replications), whereas the $\alpha1^{myc}$ subunits were observed dominantly in the ER in 78 cells (15, 19, and 44).

Thus, in the short incubation condition, the average fraction of colocalization with the membrane for $\alpha1^{myc}$ subunit

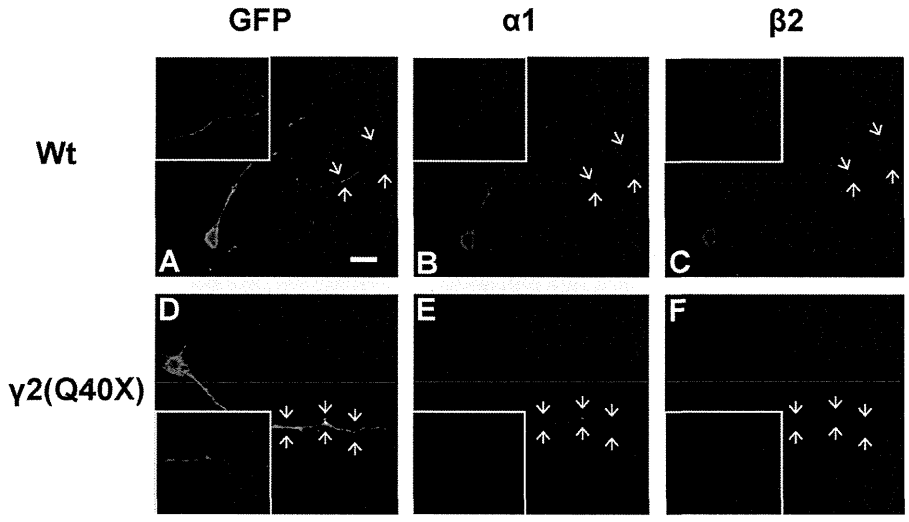

Figure 5 Axonal transport deficits of α1 and β2 subunits in neurons. Mouse hippocampal neurons were transfected with either wild type γ2 cDNAs or mutated (Q40X) cDNAs binding GFP after the IRES sequence. At 48 h after transfection, the cells were fixed, permeabilized, and stained with antibodies for GFP (green), α1 (red), and β2 (blue). Inserts are higher-magnification views of the position indicated by arrows. In neurons transfected with wild type γ2, GFP (A), α1 (B), and β2 (C), signals were strong in the axon terminals, while neurons expressing the mutated γ2 (Q40X), GFP (D), α1 (E), and β2 (F) showed lower staining intensity in their axons.

across the three replications was 24.4% for the WT receptor (26.7%, 33.3%, and 13.3% in each replication), 6.6% for the heterozygous receptors (15.4%, 4.5%, and 0%), and 2.8% for the homozygous receptor (1.6%, 6.7%, and 0%). Compared with the homozygous receptors, the WT receptors showed significantly higher colocalization with the membrane ($P = 0.029$) (Fig. 5C).

In the longer incubation condition, average fraction of colocalization with the membrane was 82% for the WT receptor (55.0%, 91.3%, and 100% in each replication), 52.9% for the heterozygous receptors (47.4%, 56.3%, and 55.2% in each replication), and 45.0% for the homozygous receptors (46.4%, 59.6% and 29.0% in each replication). Compared to the WT receptors, the homozygous receptors showed a trend to be retained in the ER ($P = 0.074$). Thus, it seems that mutant γ2 cDNAs interfered with the intracellular sorting of the receptor, resulting in its retention in the ER, even though this interference was evident only when cDNA of the mutant γ2 was injected with those of α1 and β2. These results suggest that this γ2 subunit harboring the p.Q40X mutation acts in a dominant-negative manner on intracellular trafficking of the $GABA_A$ receptor.

Axonal transport deficits of GABRA1 and GABRB2 proteins in neurons

In HEK cells, the $GABA_A$ receptor was located on the surface. To investigate whether the *GABRG2* mutant (p.Q40X) would prevent intracellular trafficking of endogenous α1 and γ2 subunits, we examined the axons of mouse hippocampal neurons in detail (Fig. 5). WT γ2 or mutated γ2 cDNA were transfected into cultured mouse hippocampal neurons and the transfected cells were identified by anti-GFP antibody. The intracellular distribution of both endogenous α1 and β2 subunits was examined by confocal microscopy after labeling with respective antibodies. The distributions of both endogenous α1 and β2 transfected mutated γ2 cDNAs were different from those of the transfected WT γ2 cDNA. In the axonal pathway, a significant portion of α1 and β2 proteins also bearing WT γ2 was distributed in the axon terminal. Interestingly, the signal intensity of both α1 and β2 subunits bearing mutant γ2 was reduced, and the signal of both subunits did not represent axon terminal. These findings suggested that the amount of transported α1 and β2 subunits was lower in neurons harboring the mutated γ2 allele compared to those with only the WT allele.

Dravet syndrome-associated *GABRG2* mutant

We next analyzed the effects of expression of the *GABRG2* mutant (p.Q40X) on the localization of α1 subunits in cultured mouse hippocampal neurons (Fig. 6). WT γ2 cDNAs transfected into mouse hippocampal neurons induced translocation of endogenous α1 subunits from the cell body to neuritic tip. In contrast, expression of the mutated γ2 (Q40X) cDNAs limited the endogenous α1 subunits to mainly the cell body. Moreover, the majority of the α1 subunits was detected on the surface of cell bodies, dendrites, and axons in neurons expressing WT γ2 cDNAs, while these units were absent at these locations in neurons expressing the mutated γ2 cDNAs. Moreover, α1 subunits partially colocalized with calnexin, another ER protein, but not with Golgi markers, GM130 and p115. However, statistical quantification regarding the distribution of the $GABA_A$ receptor in neurons could not be conducted for this study. Therefore, it cannot be definitely concluded that the γ2 subunit harboring the Q40X mutation interferes with the transportation of endogenous α1 subunits in neurons, as has been shown in the experiments with HEK cells.

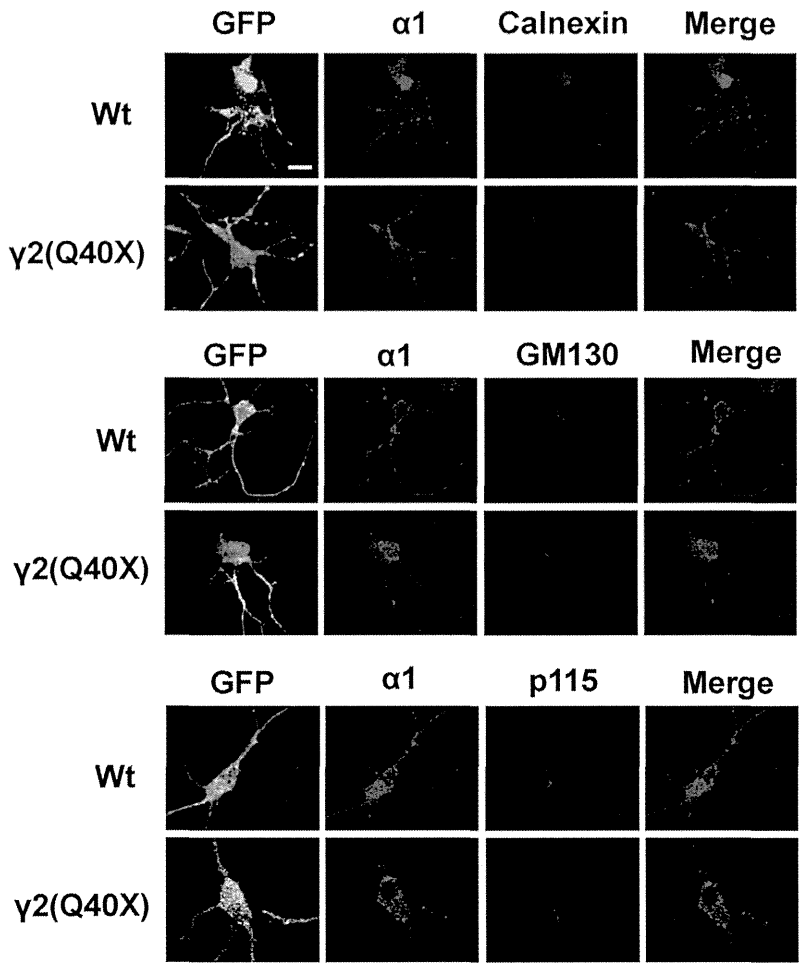

Figure 6 Accumulation of α1 and β2 subunits in ER neurons. Mouse hippocampal neurons were transfected with either wild type γ2 cDNAs or mutated (Q40X) cDNAs binding GFP after the IRES sequence. At 48 h after transfection, the cells were fixed, permeabilized, and immunostained for GFP (green) and α1 (red). An antibody to calnexin was used to mark ER (blue), while the Golgi apparatus was labeled using antibodies to GM130 and p115 (blue). In the presence of the mutated γ2 (Q40X), endogenous α1 subunits were detected mainly in the cell body. The merged images show no overlap of the subunits with GM130 or p115.

Discussion

This study provided new insight into the pathogenesis of epilepsy by showing that a nonsense mutation of *GABRG2* found in a severe epilepsy phenotype results in abnormal intracellular trafficking of $GABA_A$ receptors. We encountered twin individuals with Dravet syndrome, who had a heterozygous nonsense mutation in *GABRG2* (p.Q40X). Interestingly, this mutation was also detected in the twins' father who was asymptomatic. Electrophysiological studies in HEK cells with reconstituted $GABA_A$ receptors showed reduced GABA-induced receptor currents when mutant γ2(Q40X) protein was coexpressed with other components of the $GABA_A$ receptor, the α1 and β2 subunits. Immunohistochemical studies demonstrated the presence of mutant-positive granules in neuronal soma and neuropils, while immunocytochemical studies to determine the localization of α1 and β2 subunits showed disruption of intracellular trafficking of $GABA_A$ receptors with receptors retained in the ER following injection of mutated γ2 cDNA into the HEK cells.

The first nonsense mutation of *GABRG2*, Q351X, was reported in a male individual in a large Austrian family where a number of affected individuals showed mainly simple FS and myoclonic astatic epilepsy (Harkin et al., 2002). The Q351X mutant was expressed heterozygously in an individual whose phenotype was consistent with Dravet syndrome in a family with GEFS+. This mutation is located in the intracellular loop between the third and fourth transmembrane domains of the γ2 subunit and results in a truncated protein. Reconstituted $GABA_A$ receptor comprising WT α1 and β2 subunits and the mutant γ2 subunits in *Xenopus* oocytes showed no GABA-evoked currents. Retention of the mutant receptor in the ER was detected in HEK cells cotransfected with α1, β2, and the mutant γ2 subunits. The same mutation has been associated with both loss of function and dominant-negative suppression (Kang et al., 2009), and is located at the N-terminus of the molecule. Mutant transcripts may therefore undergo nonsense-mediated decay (NMD). A possible explanation of the molecular pathology associated with the p.Q40X mutation is haploinsufficiency caused by NMD.

However, the heterozygous *GABRG2* (+/-) gene deletion mice showed no convulsive seizures (Crestani et al., 1999). Heterozygosity of this nonsense mutation in the *GABRG2* gene in mouse may not have equivalent consequences in human, but the findings in mice raise the alternative possibility that the truncated protein caused by this mutation (p.Q40X) is actually produced and exerts a dominant-negative suppression effect on the function of the remaining WT $GABA_A$ receptors. Moreover, the proband's brain specimens immunostained against $\alpha 1$ and $\gamma 2$ subunits showed $GABA_A$ receptor harboring the mutant $\gamma 2$ (Q40X) subunit and forming aggregates in cells of the brain. These results suggest that this mutation affects the construction and intracellular sorting of the $GABA_A$ receptor molecule.

$GABA_A$ receptors are assembled at the ER and then transported to the Golgi apparatus (Connolly et al., 1996; Gorrie et al., 1997), although the majority of $GABA_A$ receptors harboring the p.Q40X mutation colocalized within the ER. The $\gamma 2$ subunits of the $GABA_A$ receptor are required for clustering of major postsynaptic $GABA_A$ receptor subtypes and trafficking of the intracellular $GABA_A$ receptor (Essrich et al., 1998; Korpi et al., 1994; Mu et al., 2002; Taylor et al., 1999, 2000). The p.Q40X mutation also interfered with the transport of $GABA_A$ receptors to the cell surface membrane.

Four mutations in *GABRG2* have thus far been associated with FS followed by childhood absence epilepsy (CAE) (Hales et al., 2005; Kang and Macdonald, 2004; Sancar and Czajkowski, 2004; Wallace et al., 2001), FS (Audenaert et al., 2006), GEFS+ (Baulac et al., 2001), and Dravet syndrome (Harkin et al., 2002). Screening for consistent electrophysiological patterns to segregate GEFS+ and Dravet syndrome have largely been unproductive (Kanai et al., 2004; Rhodes et al., 2004; Sugawara et al., 2003; Yamakawa, 2005). Although HEK293T cells transfected with mutated $\gamma 2$ subunits (p.Q40X) produced GABA-induced current amplitudes of $GABA_A$ receptors, the proband was diagnosed as Dravet syndrome. We confirmed with the experiments on HEK cells that the majority of $GABA_A$ receptors harboring the p.Q40X mutation showed heterozygous and homozygous trafficking defect with respect to translocation of the receptor and its components to the surface of cell. Although statistical quantification could not be conducted, similar findings were observed in cultivated hippocampal neurons. Thus, $GABA_A$ receptors with the mutant $\gamma 2$ subunit might be aggregated in the ER of neurons in the patients' brain. Although the proband's father harboring the same mutation was asymptomatic, the finding implicates a variable modifier, and strong candidates include factors related to the ER stress response. The association of apoptosis with certain neurological disorders was reported recently (Inoue et al., 2004; Khajavi et al., 2005), although the association of apoptosis with epilepsy has not yet been confirmed. Electrophysiological assays were performed on living cells in this study, and not on cells that had undergone apoptosis. Hence, studying the cells before any apoptotic events should allow the detection of GABA-induced current amplitudes. However, apoptotic neurons are often not found in vivo, thus explaining the appearance of phenotype as Dravet syndrome. Hence, the proband might actually have a Dravet syndrome phenotype.

In conclusion, our investigation of *GABRG2* mutation (Q40X) demonstrated the dominant-negative effects of $\alpha 1$ and $\gamma 2$ subunits. This result suggests that the differences among the phenotypes of epilepsy are likely due to the mutant $\gamma 2$ subunit. This paradigm involves a channel trafficking abnormality followed by ER accumulation. Understanding the pathogenic mechanism could provide clues to address unsolved questions about epilepsy, such as the differences between GEFS+ and Dravet syndrome. These phenotypically different entities share the same genetic abnormalities and hence are generally considered to part of a single disease spectrum or function as allelic variants.

Conflict of interest

None of the authors has any conflict of interest to disclose.

We confirm that we have read the Journal's position on issues involved in ethical publication and affirm that this report is consistent with those guidelines.

Acknowledgments

We are indebted to all members of the study family for their helpful cooperation. Ms. Minako Yonetani and Akiyo Hamachi for their technical assistance. This work was supported by a Grant-in-Aid for Young Scientists (B) (23791201 to A.I.), Grant-in-Aid for Scientific Research (A) (24249060 to S.H.), Grant-in-Aid for Challenging Exploratory Research (25670481 to S.H.), Bilateral Joint Research Projects (S.H.) from Japan Society for the Promotion of Science (JSPS), Grants for Scientific Research on Innovative Areas (221S0002 and 25129708 to A.I and S.H.) from the Ministry of Education, Culture, Sports, Science and Technology (MEXT), MEXT-supported Program for the Strategic Research Foundation at Private Universities 2013–2017 (S.H.), a Grant-in-aid for the Research on Measures for Intractable Diseases (No. H23-Nanji-Ippan-78 to S.H.) from the Ministry of Health, Labor and Welfare, Intramural Research Grant (24-7) for Neurological and Psychiatric Disorders of NCNP (S.H.), the Joint Usage/Research Program of Medical Research Institute, Tokyo Medical and Dental University (S.H.), Grants from the Mitsubishi Foundation (S.H.) and Takeda Scientific Foundation (S.H.), 2013–2017 ''Research grants for Central Research Institute for the Molecular Pathomechanisms of Epilepsy of Fukuoka University''(S.H.), Recommended Projects of Fukuoka University (117016 to S.H.), Research Grant from the Japan Foundation for Pediatric Research (A.I.), the Japan Epilepsy Research Foundation (A.I.), the Kaibara Morikazu Medical Science Promotion Foundation (A.I.), the research foundation for Clinical Medical Promotion (A.I.) and the Grant of Clinical Research Promotion Foundation (A.I.).

References

Abou-Khalil, B., Ge, Q., Desai, R., Ryther, R., Bazyk, A., Bailey, R., Haines, J.L., Sutcliffe, J.S., George Jr., A.L., 2001. Partial and generalized epilepsy with febrile seizures plus and a novel *SCN1A* mutation. Neurology 57, 2265–2272.

Audenaert, D., Schwartz, E., Claeys, K.G., Claes, L., Deprez, L., Suls, A., Van Dyck, T., Lagae, L., Van Broeckhoven, C., Macdonald, R.L., De Jonghe, P., 2006. A novel *GABRG2* mutation associated with febrile seizures. Neurology 67, 687–690.

Baulac, S., Huberfeld, G., Gourfinkel-An, I., Mitropoulou, G., Beranger, A., Prud'homme, J.F., Baulac, M., Brice, A., Bruzzone, R., LeGuern, E., 2001. First genetic evidence of GABA(A) receptor dysfunction in epilepsy: a mutation in the gamma2-subunit gene. Nat. Genet. 28, 46–48.

Brewer, G.J., Torricelli, J.R., Evege, E.K., Price, P.J., 1993. Optimized survival of hippocampal neurons in B27-supplemented neurobasal, a new serum-free medium combination. J. Neurosci. Res. 35, 567–576.

Claes, L., Ceulemans, B., Audenaert, D., Smets, K., Lofgren, A., Del-Favero, J., Ala-Mello, S., Basel-Vanagaite, L., Plecko, B., Raskin, S., Thiry, P., Wolf, N.I., Van Broeckhoven, C., De Jonghe, P., 2003. De novo *SCN1A* mutations are a major cause of severe myoclonic epilepsy of infancy. Hum. Mutat. 21, 615–621.

Claes, L., Del-Favero, J., Ceulemans, B., Lagae, L., Van Broeckhoven, C., De Jonghe, P., 2001. De novo mutations in the sodium-channel gene *SCN1A* cause severe myoclonic epilepsy of infancy. Am. J. Hum. Genet. 68, 1327–1332.

Connolly, C.N., Krishek, B.J., McDonald, B.J., Smart, T.G., Moss, S.J., 1996. Assembly and cell surface expression of heteromeric and homomeric gamma-aminobutyric acid type A receptors. J. Biol. Chem. 271, 89–96.

Crestani, F., Lorez, M., Baer, K., Essrich, C., Benke, D., Laurent, J.P., Belzung, C., Fritschy, J.M., Luscher, B., Mohler, H., 1999. Decreased GABAA-receptor clustering results in enhanced anxiety and a bias for threat cues. Nat. Neurosci. 2, 833–839.

Escayg, A., Heils, A., MacDonald, B.T., Haug, K., Sander, T., Meisler, M.H., 2001. A novel *SCN1A* mutation associated with generalized epilepsy with febrile seizures plus—and prevalence of variants in patients with epilepsy. Am. J. Hum. Genet. 68, 866–873.

Escayg, A., MacDonald, B.T., Meisler, M.H., Baulac, S., Huberfeld, G., An-Gourfinkel, I., Brice, A., LeGuern, E., Moulard, B., Chaigne, D., Buresi, C., Malafosse, A., 2000. Mutations of *SCN1A*, encoding a neuronal sodium channel, in two families with GEFS+2. Nat. Genet. 24, 343–345.

Essrich, C., Lorez, M., Benson, J.A., Fritschy, J.M., Luscher, B., 1998. Postsynaptic clustering of major $GABA_A$ receptor subtypes requires the gamma 2 subunit and gephyrin. Nat. Neurosci. 1, 563–571.

Fujiwara, T., Sugawara, T., Mazaki-Miyazaki, E., Takahashi, Y., Fukushima, K., Watanabe, M., Hara, K., Morikawa, T., Yagi, K., Yamakawa, K., Inoue, Y., 2003. Mutations of sodium channel alpha subunit type 1 (*SCN1A*) in intractable childhood epilepsies with frequent generalized tonic–clonic seizures. Brain 126, 531–546.

Fukuma, G., Oguni, H., Shirasaka, Y., Watanabe, K., Miyajima, T., Yasumoto, S., Ohfu, M., Inoue, T., Watanachai, A., Kira, R., Matsuo, M., Muranaka, H., Sofue, F., Zhang, B., Kaneko, S., Mitsudome, A., Hirose, S., 2004. Mutations of neuronal voltage-gated Na+ channel alpha 1 subunit gene *SCN1A* in core severe myoclonic epilepsy in infancy (SMEI) and in borderline SMEI (SMEB). Epilepsia 45, 140–148.

Gallagher, M.J., Shen, W., Song, L., Macdonald, R.L., 2005. Endoplasmic reticulum retention and associated degradation of a $GABA_A$ receptor epilepsy mutation that inserts an aspartate in the M3 transmembrane segment of the alpha1 subunit. J. Biol. Chem. 280, 37995–38004.

Gennaro, E., Veggiotti, P., Malacarne, M., Madia, F., Cecconi, M., Cardinali, S., Cassetti, A., Cecconi, I., Bertini, E., Bianchi, A., Gobbi, G., Zara, F., 2003. Familial severe myoclonic epilepsy of infancy: truncation of Nav1.1 and genetic heterogeneity. Epileptic Disord. 5, 21–25.

Gorrie, G.H., Vallis, Y., Stephenson, A., Whitfield, J., Browning, B., Smart, T.G., Moss, S.J., 1997. Assembly of $GABA_A$ receptors composed of alpha1 and beta2 subunits in both cultured neurons and fibroblasts. J. Neurosci. 17, 6587–6596.

Gunther, U., Benson, J., Benke, D., Fritschy, J.M., Reyes, G., Knoflach, F., Crestani, F., Aguzzi, A., Arigoni, M., Lang, Y., et al., 1995. Benzodiazepine-insensitive mice generated by targeted disruption of the gamma 2 subunit gene of gamma-aminobutyric acid type A receptors. Proc. Natl. Acad. Sci. U.S.A. 92, 7749–7753.

Hales, T.G., Tang, H., Bollan, K.A., Johnson, S.J., King, D.P., McDonald, N.A., Cheng, A., Connolly, C.N., 2005. The epilepsy mutation, gamma2(R43Q) disrupts a highly conserved inter-subunit contact site, perturbing the biogenesis of GABAA receptors. Mol. Cell. Neurosci. 29, 120–127.

Harkin, L.A., Bowser, D.N., Dibbens, L.M., Singh, R., Phillips, F., Wallace, R.H., Richards, M.C., Williams, D.A., Mulley, J.C., Berkovic, S.F., Scheffer, I.E., Petrou, S., 2002. Truncation of the GABA(A)-receptor gamma2 subunit in a family with generalized epilepsy with febrile seizures plus. Am. J. Hum. Genet. 70, 530–536.

Hirose, S., 2006. A new paradigm of channelopathy in epilepsy syndromes: intracellular trafficking abnormality of channel molecules. Epilepsy Res. 70 (1 Supplementary), S206–S217.

Hirose, S., Iwata, H., Akiyoshi, H., Kobayashi, K., Ito, M., Wada, K., Kaneko, S., Mitsudome, A., 1999. A novel mutation of *CHRNA4* responsible for autosomal dominant nocturnal frontal lobe epilepsy. Neurology 53, 1749–1753.

Hirose, S., Zenri, F., Akiyoshi, H., Fukuma, G., Iwata, H., Inoue, T., Yonetani, M., Tsutsumi, M., Muranaka, H., Kurokawa, T., Hanai, T., Wada, K., Kaneko, S., Mitsudome, A., 2000. A novel mutation of *KCNQ3* (c.925T→C) in a Japanese family with benign familial neonatal convulsions. Ann. Neurol. 47, 822–826.

Holbrook, J.A., Neu-Yilik, G., Hentze, M.W., Kulozik, A.E., 2004. Nonsense-mediated decay approaches the clinic. Nat. Genet. 36, 801–808.

Inoue, K., Khajavi, M., Ohyama, T., Hirabayashi, S., Wilson, J., Reggin, J.D., Mancias, P., Butler, I.J., Wilkinson, M.F., Wegner, M., Lupski, J.R., 2004. Molecular mechanism for distinct neurological phenotypes conveyed by allelic truncating mutations. Nat. Genet. 36, 361–369.

Ishii, A., Fukuma, G., Uehara, A., Miyajima, T., Makita, Y., Hamachi, A., Yasukochi, M., Inoue, T., Yasumoto, S., Okada, M., Kaneko, S., Mitsudome, A., Hirose, S., 2009. A de novo *KCNQ2* mutation detected in non-familial benign neonatal convulsions. Brain Dev. 31, 27–33.

Jurman, M.E., Boland, L.M., Liu, Y., Yellen, G., 1994. Visual identification of individual transfected cells for electrophysiology using antibody-coated beads. Biotechniques 17, 876–881.

Kamiya, K., Kaneda, M., Sugawara, T., Mazaki, E., Okamura, N., Montal, M., Makita, N., Tanaka, M., Fukushima, K., Fujiwara, T., Inoue, Y., Yamakawa, K., 2004. A nonsense mutation of the sodium channel gene *SCN2A* in a patient with intractable epilepsy and mental decline. J. Neurosci. 24, 2690–2698.

Kanai, K., Hirose, S., Oguni, H., Fukuma, G., Shirasaka, Y., Miyajima, T., Wada, K., Iwasa, H., Yasumoto, S., Matsuo, M., Ito, M., Mitsudome, A., Kaneko, S., 2004. Effect of localization of missense mutations in *SCN1A* on epilepsy phenotype severity. Neurology 63, 329–334.

Kanematsu, T., Jang, I.S., Yamaguchi, T., Nagahama, H., Yoshimura, K., Hidaka, K., Matsuda, M., Takeuchi, H., Misumi, Y., Nakayama, K., Yamamoto, T., Akaike, N., Hirata, M., Nakayama, K., 2002. Role of the PLC-related, catalytically inactive protein p130 in GABA(A) receptor function. EMBO J. 21, 1004–1011.

Kang, J.Q., Macdonald, R.L., 2004. The $GABA_A$ receptor gamma2 subunit R43Q mutation linked to childhood absence epilepsy and febrile seizures causes retention of alpha1beta2gamma2S receptors in the endoplasmic reticulum. J. Neurosci. 24, 8672–8677.

Kang, J.Q., Shen, W., Macdonald, R.L., 2009. The GABRG2 mutation, Q351X, associated with generalized epilepsy with febrile seizures plus, has both loss of function and dominant-negative suppression. J. Neurosci. 29, 2845–2856.

Keller, C.A., Yuan, X., Panzanelli, P., Martin, M.L., Alldred, M., Sassoe-Pognetto, M., Luscher, B., 2004. The gamma2 subunit of

GABA(A) receptors is a substrate for palmitoylation by GODZ. J. Neurosci. 24, 5881–5891.

Khajavi, M., Inoue, K., Wiszniewski, W., Ohyama, T., Snipes, G.J., Lupski, J.R., 2005. Curcumin treatment abrogates endoplasmic reticulum retention and aggregation-induced apoptosis associated with neuropathy-causing myelin protein zero-truncating mutants. Am. J. Hum. Genet. 77, 841–850.

Kimura, K., Sugawara, T., Mazaki-Miyazaki, E., Hoshino, K., Nomura, Y., Tateno, A., Hachimori, K., Yamakawa, K., Segawa, M., 2005. A missense mutation in *SCN1A* in brothers with severe myoclonic epilepsy in infancy (SMEI) inherited from a father with febrile seizures. Brain Dev. 27, 424–430.

Kittler, J.T., McAinsh, K., Moss, S.J., 2002. Mechanisms of $GABA_A$ receptor assembly and trafficking: implications for the modulation of inhibitory neurotransmission. Mol. Neurobiol. 26, 251–268.

Kittler, J.T., Rostaing, P., Schiavo, G., Fritschy, J.M., Olsen, R., Triller, A., Moss, S.J., 2001. The subcellular distribution of GABARAP and its ability to interact with NSF suggest a role for this protein in the intracellular transport of GABA(A) receptors. Mol. Cell. Neurosci. 18, 13–25.

Kneussel, M., 2002. Dynamic regulation of GABA(A) receptors at synaptic sites. Brain Res. Brain Res. Rev. 39, 74–83.

Korpi, E.R., Kuner, T., Kristo, P., Kohler, M., Herb, A., Luddens, H., Seeburg, P.H., 1994. Small N-terminal deletion by splicing in cerebellar alpha 6 subunit abolishes $GABA_A$ receptor function. J. Neurochem. 63, 1167–1170.

Macdonald, R.L., Gallagher, M.J., Feng, H.J., Kang, J., 2004. GABA(A) receptor epilepsy mutations. Biochem. Pharmacol. 68, 1497–1506.

Moss, S.J., Smart, T.G., 2001. Constructing inhibitory synapses. Nat. Rev. 2, 240–250.

Mu, W., Cheng, Q., Yang, J., Burt, D.R., 2002. Alternative splicing of the GABA(A) receptor alpha 4 subunit creates a severely truncated mRNA. Brain Res. Bull. 58, 447–454.

Mulley, J.C., Scheffer, I.E., Petrou, S., Dibbens, L.M., Berkovic, S.F., Harkin, L.A., 2005. *SCN1A* mutations and epilepsy. Hum. Mutat. 25, 535–542.

Nabbout, R., Gennaro, E., Dalla Bernardina, B., Dulac, O., Madia, F., Bertini, E., Capovilla, G., Chiron, C., Cristofori, G., Elia, M., Fontana, E., Gaggero, R., Granata, T., Guerrini, R., Loi, M., La Selva, L., Lispi, M.L., Matricardi, A., Romeo, A., Tzolas, V., Valseriati, D., Veggiotti, P., Vigevano, F., Vallee, L., Dagna Bricarelli, F., Bianchi, A., Zara, F., 2003. Spectrum of *SCN1A* mutations in severe myoclonic epilepsy of infancy. Neurology 60, 1961–1967.

Ohmori, I., Ouchida, M., Ohtsuka, Y., Oka, E., Shimizu, K., 2002. Significant correlation of the *SCN1A* mutations and severe myoclonic epilepsy in infancy. Biochem. Biophys. Res. Commun. 295, 17–23.

Rhodes, T.H., Lossin, C., Vanoye, C.G., Wang, D.W., George Jr., A.L., 2004. Noninactivating voltage-gated sodium channels in severe myoclonic epilepsy of infancy. Proc. Natl. Acad. Sci. U.S.A. 101, 11147–11152.

Sancar, F., Czajkowski, C., 2004. A $GABA_A$ receptor mutation linked to human epilepsy (gamma2R43Q) impairs cell surface expression of alphabetagamma receptors. J. Biol. Chem. 279, 47034–47039.

Sarto, I., Wabnegger, L., Dogl, E., Sieghart, W., 2002. Homologous sites of GABA(A) receptor alpha(1), beta(3) and gamma(2) subunits are important for assembly. Neuropharmacology 43, 482–491.

Shi, X., Yasumoto, S., Nakagawa, E., Fukasawa, T., Uchiya, S., Hirose, S., 2009. Missense mutation of the sodium channel gene SCN2A causes Dravet syndrome. Brain Dev. 31, 758–762.

Singh, R., Andermann, E., Whitehouse, W.P., Harvey, A.S., Keene, D.L., Seni, M.H., Crossland, K.M., Andermann, F., Berkovic, S.F., Scheffer, I.E., 2001. Severe myoclonic epilepsy of infancy: extended spectrum of GEFS+? Epilepsia 42, 837–844.

Sugawara, T., Mazaki-Miyazaki, E., Fukushima, K., Shimomura, J., Fujiwara, T., Hamano, S., Inoue, Y., Yamakawa, K., 2002. Frequent mutations of *SCN1A* in severe myoclonic epilepsy in infancy. Neurology 58, 1122–1124.

Sugawara, T., Mazaki-Miyazaki, E., Ito, M., Nagafuji, H., Fukuma, G., Mitsudome, A., Wada, K., Kaneko, S., Hirose, S., Yamakawa, K., 2001. Nav1.1 mutations cause febrile seizures associated with afebrile partial seizures. Neurology 57, 703–705.

Sugawara, T., Tsurubuchi, Y., Fujiwara, T., Mazaki-Miyazaki, E., Nagata, K., Montal, M., Inoue, Y., Yamakawa, K., 2003. Nav1.1 channels with mutations of severe myoclonic epilepsy in infancy display attenuated currents. Epilepsy Res. 54, 201–207.

Taylor, P.M., Connolly, C.N., Kittler, J.T., Gorrie, G.H., Hosie, A., Smart, T.G., Moss, S.J., 2000. Identification of residues within GABA(A) receptor alpha subunits that mediate specific assembly with receptor beta subunits. J. Neurosci. 20, 1297–1306.

Taylor, P.M., Thomas, P., Gorrie, G.H., Connolly, C.N., Smart, T.G., Moss, S.J., 1999. Identification of amino acid residues within GABA(A) receptor beta subunits that mediate both homomeric and heteromeric receptor expression. J. Neurosci. 19, 6360–6371.

Ueno, S., Bracamontes, J., Zorumski, C., Weiss, D.S., Steinbach, J.H., 1997. Bicuculline and gabazine are allosteric inhibitors of channel opening of the $GABA_A$ receptor. J. Neurosci. 17, 625–634.

Wallace, R.H., Hodgson, B.L., Grinton, B.E., Gardiner, R.M., Robinson, R., Rodriguez-Casero, V., Sadleir, L., Morgan, J., Harkin, L.A., Dibbens, L.M., Yamamoto, T., Andermann, E., Mulley, J.C., Berkovic, S.F., Scheffer, I.E., 2003. Sodium channel alpha1-subunit mutations in severe myoclonic epilepsy of infancy and infantile spasms. Neurology 61, 765–769.

Wallace, R.H., Marini, C., Petrou, S., Harkin, L.A., Bowser, D.N., Panchal, R.G., Williams, D.A., Sutherland, G.R., Mulley, J.C., Scheffer, I.E., Berkovic, S.F., 2001. Mutant GABA(A) receptor gamma2-subunit in childhood absence epilepsy and febrile seizures. Nat. Genet. 28, 49–52.

Wang, H., Bedford, F.K., Brandon, N.J., Moss, S.J., Olsen, R.W., 1999. GABA(A)-receptor-associated protein links GABA(A) receptors and the cytoskeleton. Nature 397, 69–72.

Yamakawa, K., 2005. Epilepsy and sodium channel gene mutations: gain or loss of function? Neuroreport 16, 1–3.

ELSEVIER

Brain & Development 36 (2014) 21–27

BRAIN & DEVELOPMENT
Official Journal of the Japanese Society of Child Neurology

www.elsevier.com/locate/braindev

Original article

Magnetoencephalography localizing spike sources of atypical benign partial epilepsy

Hideaki Shiraishi [a], Kazuhiro Haginoya [b], Eiji Nakagawa [c], Shinji Saitoh [a], Yutaka Kaneko [d], Nobukazu Nakasato [e], Derrick Chan [f,g], Hiroshi Otsubo [f,*]

[a] *Department of Pediatrics, Hokkaido University Graduate School of Medicine, Sapporo, Hokkaido, Japan*
[b] *Department of Pediatrics, Tohoku University School of Medicine, Sendai, Miyagi, Japan*
[c] *Department of Neurology, National Hospital for Mental, Nervous and Muscular Disorders, National Center of Neurology and Psychiatry, Kodaira, Tokyo, Japan*
[d] *Department of Neurosurgery, National Hospital for Mental, Nervous and Muscular Disorders, National Center of Neurology and Psychiatry, Kodaira, Tokyo, Japan*
[e] *Department of Epileptology, Tohoku University School of Medicine, Sendai, Miyagi, Japan*
[f] *Division of Neurology, The Hospital for Sick Children, University of Toronto, Toronto, Ontario, Canada*
[g] *Neurology Service, Department of Pediatric Medicine, KK Women's and Children's Hospital, Singapore*

Received 25 September 2012; received in revised form 24 December 2012; accepted 25 December 2012

Abstract

Rationale: Atypical benign partial epilepsy (ABPE) is characterized by centro-temporal electroencephalography (EEG) spikes, continuous spike and waves during sleep (CSWS), and multiple seizure types including epileptic negative myoclonus (ENM), but not tonic seizures. This study evaluated the localization of magnetoencephalography (MEG) spike sources (MEGSSs) to investigate the clinical features and mechanism underlying ABPE. *Methods:* We retrospectively analyzed seizure profiles, scalp video EEG (VEEG) and MEG in ABPE patients. *Results:* Eighteen ABPE patients were identified (nine girls and nine boys). Seizure onset ranged from 1.3 to 8.8 years (median, 2.9 years). Initial seizures consisted of focal motor seizures (15 patients) and absences/atypical absences (3). Seventeen patients had multiple seizure types including drop attacks (16), focal motor seizures (16), ENM (14), absences/atypical absences (11) and focal myoclonic seizures (10). VEEG showed centro-temporal spikes and CSWS in all patients. Magnetic resonance imaging (MRI) was reported as normal in all patients. MEGSSs were localized over the following regions: both Rolandic and sylvian (8), peri-sylvian (5), peri-Rolandic (4), parieto-occipital (1), bilateral (10) and unilateral (8). All patients were on more than two antiepileptic medications. ENM and absences/atypical absences were controlled in 14 patients treated with adjunctive ethosuximide. *Conclusion:* MEG localized the source of centro-temporal spikes and CSWS in the Rolandic-sylvian regions. Centro-temporal spikes, Rolandic-sylvian spike sources and focal motor seizures are evidence that ABPE presents with Rolandic-sylvian onset seizures. ABPE is therefore a unique, age-related and localization-related epilepsy with a Rolandic-sylvian epileptic focus plus possible thalamo-cortical epileptic networks in the developing brain of children.

Keywords: Epileptic negative myoclonus; Focal seizure; Atypical absence; Centro-temporal spike; Continuous spike and waves during sleep; Secondary bilateral synchrony

* Corresponding author. Address: Division of Neurology, The Hospital for Sick Children, 555 University Avenue, University of Toronto, Toronto, ON, Canada M5G 1X8. Tel.: +1 416 813 6660; fax: +1 416 813 6334.
E-mail addresses: hiotsubo@rogers.com, hiroshi.otsubo@sickkids.ca (H. Otsubo).

0387-7604/$ - see front matter
http://dx.doi.org/10.1016/j.braindev.2012.12.011

1. Introduction

Atypical benign partial epilepsy in childhood (ABPE) initially presents with the following signs and symptoms: (i) onset age of 2.5–6 years; (ii) multiple seizure types including focal motor, atypical absences and myoclonic-atonic seizures; (iii) electroencephalography (EEG) showing central and mid-temporal spikes and diffuse slow spike-wave activities during drowsiness or sleep; and (iv) normal development or mild mental retardation [1]. Despite multiple seizure types and slow spike and waves on EEG, ABPE is distinguished from Lennox–Gastaut syndrome by its characteristic spontaneous remission, lack of tonic seizures or developmental delay, and normal awake EEG background activity. Since hemi-convulsive seizures during sleep and contralateral/bilateral centro-temporal epileptiform discharges are present at the beginning, the electro-clinical findings of ABPE are indistinguishable from those of benign epilepsy with centro-temporal spikes (BECTS) [2–5]. BECTS is the most well-recognized, age-related idiopathic focal epilepsy with occasional epileptic seizures despite frequent centro-temporal spikes on EEG. In contrast, ABPE patients tend to develop atypical absences or myoclonic-atonic seizures during the course of their condition. Tovia et al. [6] showed that 0.5% of patients with BECTS were categorized as atypical variants, while Doose et al. [7] found that 29% of the relatives of ABPE patients had some abnormal activities on EEG. Finally, Gobbi et al. [8] reviewed several subtypes of idiopathic focal epilepsies to categorize ABPE as a "Rolandic epilepsy-related disorder"; these age-related epilepsies including ABPE and BECTS were attributed to a maturational continuum with different manifestations.

Epileptic negative myoclonus (ENM) is one of the characteristic seizure patterns in ABPE. Oguni et al. [6] analyzed the ictal EEG findings of ENM and demonstrated generalized, bilateral synchronous discharges, while ictal magnetoencephalography (MEG) of an ABPE patient showed that the spike sources of ENM were localized at the peri-sylvian region [7].

MEG is a relatively new clinical technique that uses superconducting quantum interference devices (SQUIDs) to measure and localize sources of extracranial magnetic fields generated by intraneuronal electric currents. Current MEG machines have a whole-head array of more than 100 sensors contained within a helmet-shaped Dewar, which effectively covers most of the brain surface. MEG has been increasingly used for localization of the epileptic zone and functional mapping in epilepsy patients. MEG in BECTS patients showed spike sources with an anterior–posterior oriented perpendicular to the Rolandic fissure [8,9]. No case series of ABPE have thus far used MEG to localize epileptic spike sources.

We conducted a multi-center study to collect clinical, EEG and MEG findings in ABPE patients, with MEG used to characterize the spike sources (MEGSSs) in ABPE. We hypothesize that the epileptic network in ABPE is localized in both the Rolandic-sylvian cortex and thalamo-cortical networks, based on their unique clinical and electrophysiological features.

2. Patients and methods

We collaborated with four institutions on this study: the Department of Pediatrics, Hokkaido University School of Medicine (HU); Department of Pediatrics, Tohoku University School of Medicine (TU); Department of Pediatrics, National Center of Neurology and Psychiatry (NCNP), Japan; and the Division of Neurology, The Hospital for Sick Children (HSC), Toronto, Ontario, Canada.

2.1. Patients

We studied 18 patients with ABPE (nine females and nine males). We diagnosed ABPE according to the triad of diagnostic criteria as follows: (1) focal motor seizures, absences/atypical absences, atonic seizures including ENM, myoclonic seizures and drop attacks described by parents; (2) EEG findings of central and middle temporal spikes and generalized slow spike-wave activity during drowsiness or sleep similar to continuous spike and slow waves during sleep (CSWS); (3) normal development or mild mental retardation during the clinical course.

2.2. EEG

Scalp video EEGs were recorded using the international 10-20 electrode placement system and electromyography (EMG) electrodes for bilateral deltoid muscles to capture ENM. Awake and sleep EEGs were recorded in all patients.

2.3. MEG and magnetic resonance imaging

Initial MEG studies were conducted at the onset of ENM. Seven patients had multiple MEG studies up to six times. Parents or guardians of all patients provided written informed consent for the MEG studies. MEG and EEG were done in a magnetically shielded room. MEG was recorded using a system with 306 SQUIDs (Vectorview; Elekta-Neuromag Ltd., Helsinki, Finland) at HU, NCNP and TU, and with an Omega system (151 channels, VSM MedTech Ltd., Port Coquitlam, BC, Canada) at HSC. MEG data were recorded with a band pass filter of 0.03–133 Hz at HU, NCNP and TU, and of 1–208 Hz at HSC. Sampling frequency was 400 Hz at HU, 600 Hz at NCNP and TU, and 625 Hz at HSC. EEGs were recorded using the international 10-20 system, with additional electrocardiogram (ECG)

electrodes. MEG data were recorded for >1 h per patient, collecting data in 4-min blocks at HU, NCNP and TU. At HSC, MEG was recorded in 15 two-minute blocks for a total of 30 min [10]. Patients were lying in the supine position. Sedative agents were used for uncooperative patients. The relative position of the head and the MEG sensors were determined by attaching three small head-position indicator coils to the head. The positions of the coils were digitized and subsequently recorded by the MEG sensors for co-registration with 1.5 T (tesla)/3 T magnetic resonance image (MRI) with high-resolution sequences.

2.4. MEG source analysis

MEG data were digitally filtered using a band filter of 3–30 Hz at HU, NCNP and TU, or at 3–70 Hz at HSC for offline analysis. Segments containing abnormal paroxysms were selected manually. Individual spikes were analyzed to localize the spike source per spike using an equivalent current dipole (ECD) model or dynamic statistical parametric mapping (dSPM) [11,12].

3. Results

3.1. Seizure profiles (Table 1)

Seizure onsets ranged from 1.3 to 8.8 years with a median age of 2.9 years. The seizures started as focal motor seizures in 15 patients (83%) and absences/atypical absences in three patients (17%).

All patients except one patient had multiple types of seizures in their seizure histories. Drop attacks, in which the precise seizure type remains unknown, were most common (16 patients, 89%). One patient (Patient 17) presented with a history of only drop attack seizures. Focal motor seizures (16 patients, 89%), ENM (14 patients, 78%), absences/atypical absences (11 patients, 61%), myoclonic seizures (10 patients, 56%) and secondarily generalized tonic-clonic seizures (nine patients, 50%) were seen in more than half of the patients (Supplementary videos 1 and 2). Focal sensory seizures (six patients, 33%) and epileptic spasms (two patients, 11%) were also reported.

Table 1
Seizure profiles.

Seizure onset	1.3–8.8 years (median, 2.9 years)	
Initial seizures	Focal motor seizures	15 (83%)
	Absences/atypical absences	3 (17%)
Type of seizures in patient history	Drop attacks	16 (89%)
	Focal motor seizures	16 (89%)
	Epileptic negative myoclonus	14 (78%)
	Absences/atypical absences	11 (61%)
	Myoclonic seizures	10 (56%)
	Secondarily generalized tonic-clonic seizures	9 (50%)
	Focal sensory seizures	6 (33%)
	Epileptic spasms	2 (11%)

3.2. Past and family history

There was no past history of epilepsy before the seizure onset in any of the 18 patients, while three patients (17%) had a positive family history of febrile seizures.

3.3. Cognitive functions

Cognitive function was evaluated in 15 patients. All 15 patients had the evaluations while they presented with ENM. A developmental quotient results ranged from 54 to 85 in five patients. The full-scale intelligence quotient test (Wechsler Intelligence Scale for Children) results ranged from 53 to 103 in 10 patients.

3.4. MRI

No patient showed an abnormality on MRI.

3.5. EEG (Fig. 1)

EEG showed interictal centro-temporal spikes in all 18 patients. Continuous generalized and/or centro-temporal spike and waves during sleep were also noticed in all patients. When video EEG captured ENM, generalized high-amplitude spike or polyspikes, and waves were associated with a brief attenuation of EMG activities corresponding to muscle atonia in 12 patients (Supplementary video 1). Absences/atypical absences showed generalized and irregular spike and slow waves around 3 Hz on EEG in 16 patients (Supplementary video 2).

3.6. MEG (Fig. 2 and Table 2)

MEG localized MEGSSs over both Rolandic and sylvian fissures in eight patients, the peri-sylvian region alone in five patients, and the peri-Rolandic region alone in four patients. One patient had MEGSSs in the left parieto-occipital region, even though EEG showed left centro-temporal spikes (Patient 6). Most spike sources were oriented perpendicularly to either the Rolandic or sylvian fissure. The spike sources demonstrated identical orientations in 11 patients (61%). MEGSSs were located in bilateral hemispheres in 10 patients (56%) and in a

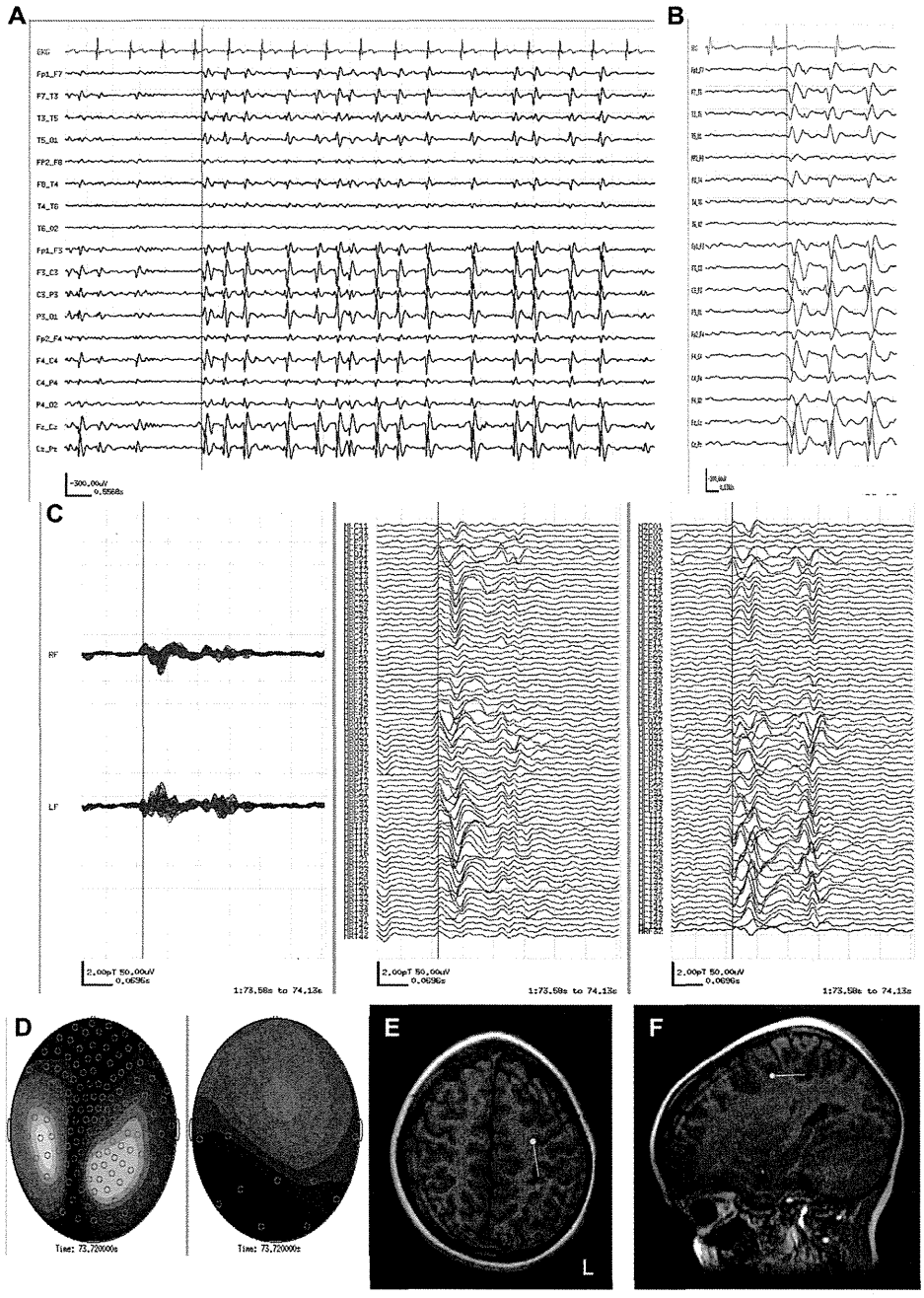

Fig. 1. MEG and EEG in case 18. (A) A–P bipolar EEG shows continuous spike and waves during sleep at the time of MEG study (low frequency filter, 3 Hz; high frequency filter, 70 Hz). (B) The same EEG of A is expanded to demonstrate left centro-temporal spikes preceding to the right central spikes after the red cursor. (C) 151 MEG channels are labeled by two colors (red for right hemisphere and blue for left hemisphere), and show the view of overlay (left), right channels (middle), and left channels (right). MEG shows more complex polyspikes than EEG on the overlay left channels. Note the MEG spikes (red cursor) leading to EEG spikes (behind the red cursor) on B. (D) MEG topography (left) and EEG topography (right). Note that magnetic and electric topographies are perpendicular to each other. (E) Axial MRI shows MEG spike source at the time of red cursor at the left Rolandic region (circle, position; tail, orientation, and moment). (F) Sagittal MRI shows the same MEG spike source of (E) at the left Rolandic region. The equivalent current dipole (spike source) is oriented horizontally, projecting negativity towards the frontal region and positivity towards the parietal region, corresponding to the EEG topography (D, right). (For interpretation of color in Fig. 1, the reader is referred to the web version of this article)

unilateral hemisphere in eight patients (44%). In all 10 patients with bilateral MEGSS, the MEGSS showed identical patterns and locations in the both hemispheres. ECD could not be estimated in one patient due to diffuse right hemispheric discharges without leading spikes. Therefore, we applied dSPM and localized the MEGSSs in the right sylvian fissure (Patient 7). Seven patients underwent multiple MEG studies. Six patients with

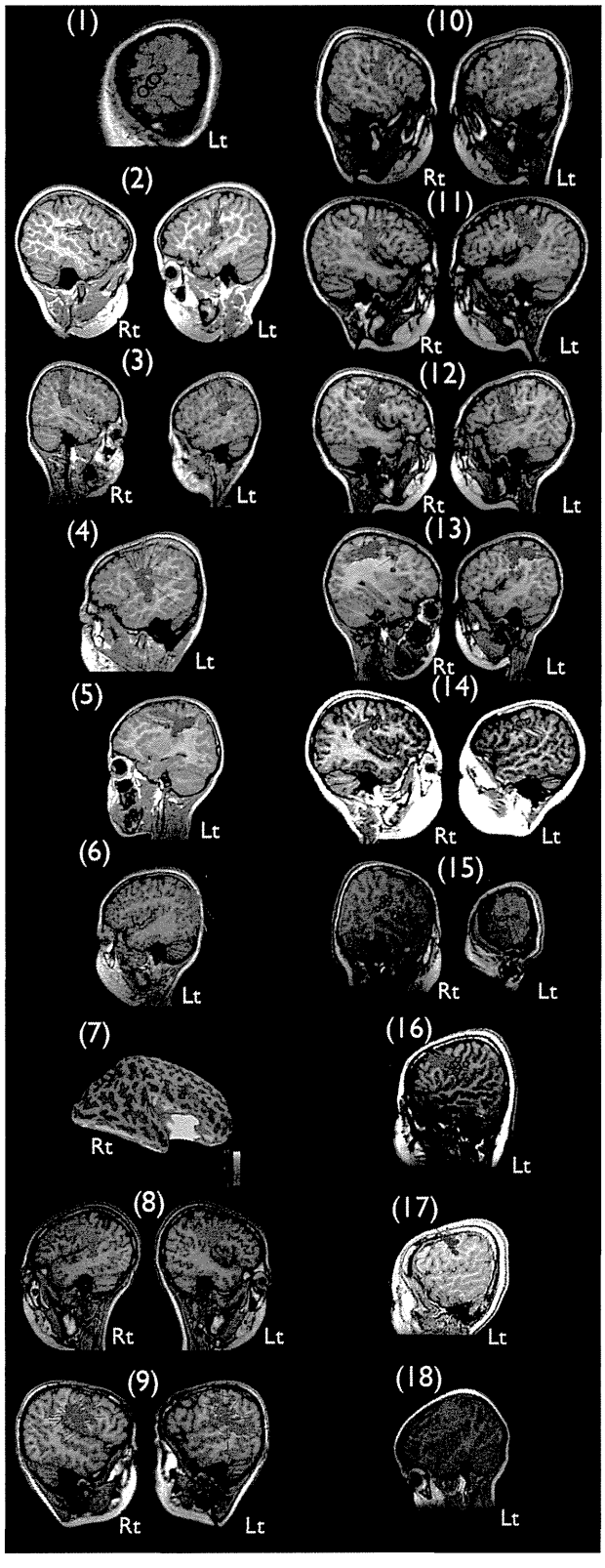

Fig. 2. MRI with MEG spike sources in 18 cases. Red circles demonstrate the source of MEG spikes. Tails indicate orientations and moments of the MEG spike sources. Case 7 shows dynamic statistical parametric mapping. The color bar indicates the P value, ranging from gray, 1×10^{-1} to yellow, $1 \times 10^{-4.3}$. (For interpretation of color in Fig. 1, the reader is referred to the web version of this article)

bilateral MEGSS became unilateral MEGSS. One patient showed consistent unilateral MEGSS. Six patients showed no MEGSS at the last MEG study when they were seizure free.

3.7. Treatments

All 18 patients were administered multiple antiepileptic medications ranging from 2 to 12 medications (mean 5.8) during their courses. Ethosuximide (ESM) succeeded in controlling various seizure types of ABPE, especially ENM and absences/atypical absences in 14 patients (78%); of these, all achieved seizure freedom after ESM was started, and 11 (89%) of the 14 were still on ESM at the last follow-up. Two of three patients in whom ESM was discontinued were no longer on any antiepileptic medication. CBZ was initially started in 16 patients (89%), but 14 (88%) experienced worsening of seizures after CBZ was initiated, and the treatment was discontinued. Two patients were seizure free on a combination of CBZ and ESM (Patient 6) or CBZ, ZNS and CLB (Patient 8). Valproic acid (VPA) was tried in 16 (89%) patients, and six of these (38%) were still on VPA at the last follow-up. Other medications tried included zonisamide (10 patients, 56%), clobazam (10 patients, 56%), clonazepam (eight patients, 44%) acetazolamide (five patients, 28%), phenytoin (five patients, 28%) and diazepam (four patients, 22%). The medications still being used at the last follow-up consisted of zonisamide in 3/10 patients (30%), clobazam in 4/10 patients (40%), clonazepam in 3/8 patients (38%), acetazolamide in 2/5 patients (40%) and diazepam in 2/4 patients (50%).

Two patients underwent epilepsy surgery. Patient 8 underwent cortical excision over the left supra-marginal gyrus at the age of 12 years. Surgical pathology revealed microdysgenesis with increased ganglion cells. She achieved 75–90% seizure reduction after the surgery, and was seizure free on three medications at 17.5 years old. Anterior two-thirds corpus callosotomy was performed at the age of 6 years for drop attacks in Patient 9. The patient was seizure free on two medications at 10 years old.

3.8. Seizure outcome

The age at last follow-up of the 18 patients ranged from 5.4 to 17.5 years (median 11.8 years). All were seizure free, two patients (11%) without any medication. Five patients (28%) were only on one medication, including four patients with ESM. The remaining 11 patients had multiple medications; six were on two medications, four were on three medications, and one patient was on four medications. Among seven patients with multiple MEG studies, medication changes, cognitive results effected less prominent for MEGSS than seizure improvements.

4. Discussion

MEG localized a Rolandic-sylvian epileptic focus of ABPE.

In ABPE, interictal MEG revealed localized clusters of spike sources around the Rolandic-sylvian fissures corresponding to both centro-temporal spikes and CSWS on EEG. The identically clustered Rolandic-sylvian MEGSSs of interictal epileptic discharges in patients with ABPE suggested that the epileptic focus was located around the Rolandic-sylvian regions involving the motor cortex in most cases. In our series, the peri-sylvian region MEGSSs were also recorded in 13 of 18 ABPE patients. In contrast, MEGSSs in BECTS were specifically localized along the Rolandic region with definite identical orientations vertical to the central sulcus [8,9]. In the older children with BECTS, MEGSSs shifted to the lower part of the Rolandic region close to the operculum.

Kubota et al. [10] reported an ictal MEG study localizing the spike source of ENM with generalized EEG spikes at the sylvian fissure in one ABPE patient [7]. ENM was characterized by spike or polyspikes on EEG time-locked to attenuation of EMG activity, which corresponded to muscle atonia [6]. Series of ENM often caused atonic seizures. Both interictal and ictal MEGSSs indicate that a subset of the epileptogenic zones responsible for focal seizures and ENM in ABPE patients is localized around the Rolandic-sylvian regions. In contrast, MEGSSs in three patients with Lennox–Gastaut syndrome with ENM were localized over inconsistent and various brain regions that did not include the Rolandic-sylvian regions [13].

Table 2
MEG spike source localization.

Patients	Regions			Hemispheres	
	Rolandic	Sylvian	Other lobe	Bilateral	Unilateral
1		1			1
2	1	1		1	
3		1		1	
4		1			1
5	1				1
6			Occipital		1
7		1			1
8	1	1		1	
9	1	1		1	
10		1		1	
11	1	1		1	
12	1	1		1	
13	1	1		1	
14	1			1	
15	1	1		1	
16	1				1
17	1				1
18	1	1			1
Total	12	13		10	8

Fifteen of eighteen patients in this series presented with focal motor seizures at the onset, and these persisted in addition to multiple other seizure types developing in 16 patients. ABPE might also be confused diagnostically with BECTS as ABPE appears superficially similar on scalp EEG and also presents with focal motor seizures. In ABPE patients, MEGSS extended to peri-sylvian region in addition to Rolandic region or localized even peri-sylvian region alone.

4.1. MEG localized spike dipoles in CSWS of ABPE

Sleep EEG often shows almost-continuous generalized or centro-temporal spike and waves during sleep in ABPE patients, resembling CSWS. Another differential diagnosis of ABPE is epileptic encephalopathy with CSWS (ECSWS), and there are no reports of source localizations using MEG in patients with ECSWS. The role of MEG remains to be explored in this entity. Kelemen et al. [17] reported three patients with CSWS secondary to destructive lesions in the thalamus [14], and CSWS development was often observed in patients with a thalamic lesion, indicative of thalamo-cortical dysfunction with an epileptic network [15,16]. ESM can be efficacious for seizures in ABPE patients, especially for ENM [6]. In 13 (72%) of the 18 ABPE patients studied herein, ESM completely suppressed their ENM. In other studies, systemic administration of ESM significantly reduced spike and wave discharges in genetic absence epilepsy models [17–19]. Continuous and generalized slow spike and waves during sleep in patients with ECSWS have been associated with secondary bilateral synchrony with leading foci [20,21]. The CSWS in ABPE could also be due to secondary bilateral synchrony, but originating specifically from the Rolandic-sylvian regions. The effect of ESM on the clinical seizures and CSWS indicates that the epileptic substitute of thalamic and Rolandic-sylvian networks produce ABPE.

Patry et al. [22] reported six patients with ECSWS, and heterogeneous seizure types of ECSWS that comprise focal motor seizures, absences, and epileptic falls while awake [21] resemble those of ABPE. Consequently, it can be difficult to distinguish ABPE from ECSWS clinically not analyzing the localization of epileptic foci. Further investigation of MEG in ECSWS may therefore serve to differentiate epileptic sources in these patients and improve our understanding of the epileptic networks and mechanisms leading to the observed cognitive disabilities.

5. Conclusions

MEG localized spike dipoles of centro-temporal spikes and CSWS over the Rolandic-sylvian regions in ABPE, indicating that ABPE is the localization-related

epilepsy with Rolandic-sylvian onset seizures. In addition, the effects of ESM on ENM and atypical absences suggest the involvement of thalamo-cortical circuitry in the epileptic network. ABPE is a unique age-related epilepsy involving the Rolandic-sylvian plus thalamo-cortical networks in the developing brain of children.

Disclosure of conflicts of interest

The authors have no financial or personal relations that could pose a conflict of interest.

Acknowledgment

We confirm that we have read the Journal's position on issues involved in ethical publication and affirm that this report is consistent with those guidelines.

Appendix A. Supplementary data

Supplementary data associated with this article can be found, in the online version, at http://dx.doi.org/10.1016/j.braindev.2012.12.011.

References

[1] Aicardi J, Chevrie JJ. Atypical benign partial epilepsy of childhood. Dev Med Child Neurol 1982;24:281–92.
[2] Beaumanoir A, Ballis T, Varfis G, Ansari K. Benign epilepsy of childhood with Rolandic spikes. A clinical, electroencephalographic, and telencephalographic study. Epilepsia 1974;15:301–15.
[3] Bernardina BD, Tassinari CA. EEG of a nocturnal seizure in a patient with "benign epilepsy of childhood with Rolandic spikes". Epilepsia 1975;16:497–501.
[4] Blom S, Heijbel J. Benign epilepsy of children with centro-temporal EEG foci. Discharge rate during sleep. Epilepsia 1975;16:133–40.
[5] Fejerman N, Caraballo R, Tenembaum SN. Atypical evolutions of benign localization-related epilepsies in children: are they predictable? Epilepsia 2000;41:380–90.
[6] Oguni H, Uehara T, Tanaka T, Sunahara M, Hara M, Osawa M. Dramatic effect of ethosuximide on epileptic negative myoclonus: implications for the neurophysiological mechanism. Neuropediatrics 1998;29:29–34.
[7] Kubota M, Nakura M, Hirose H, Kimura I, Sakakihara Y. A magnetoencephalographic study of negative myoclonus in a patient with atypical benign partial epilepsy. Seizure: J Br Epilepsy Assoc 2005;14:28–32.
[8] Minami T, Tasaki K, Yamamoto T, Gondo K, Yanai S, Ueda K. Magneto-encephalographical analysis of focal cortical heterotopia. Dev Med Child Neurol 1996;38:945–9.
[9] Ishitobi M, Nakasato N, Yamamoto K, Iinuma K. Opercular to interhemispheric source distribution of benign Rolandic spikes of childhood. NeuroImage 2005;25:417–23.
[10] RamachandranNair R, Otsubo H, Shroff MM, Ochi A, Weiss SK, Rutka JT, et al. MEG predicts outcome following surgery for intractable epilepsy in children with normal or nonfocal MRI findings. Epilepsia 2007;48:149–57.
[11] Dale AM, Liu AK, Fischl BR, Buckner RL, Belliveau JW, Lewine JD, et al. Dynamic statistical parametric mapping: combining fMRI and MEG for high-resolution imaging of cortical activity. Neuron 2000;26:55–67.
[12] Shiraishi H, Ahlfors SP, Stufflebeam SM, Takano K, Okajima M, Knake S, et al. Application of magnetoencephalography in epilepsy patients with widespread spike or slow-wave activity. Epilepsia 2005;46:1264–72.
[13] Sakurai K, Tanaka N, Kamada K, Takeuchi F, Takeda Y, Koyama T. Magnetoencephalographic studies of focal epileptic activity in three patients with epilepsy suggestive of Lennox–Gastaut syndrome. Epileptic Disord 2007;9:158–63.
[14] Kelemen A, Barsi P, Gyorsok Z, Sarac J, Szucs A, Halasz P. Thalamic lesion and epilepsy with generalized seizures, ESES and spike-wave paroxysms – report of three cases. Seizure: J Br Epilepsy Assoc 2006;15:454–8.
[15] Battaglia D, Veggiotti P, Lettori D, Tamburrini G, Tartaglione T, Graziano A, et al. Functional hemispherectomy in children with epilepsy and CSWS due to unilateral early brain injury including thalamus: sudden recovery of CSWS. Epilepsy Res 2009;87:290–8.
[16] Guzzetta F, Battaglia D, Veredice C, Donvito V, Pane M, Lettori D, et al. Early thalamic injury associated with epilepsy and continuous spike-wave during slow sleep. Epilepsia 2005;46:889–900.
[17] Hanaya R, Sasa M, Ujihara H, Fujita Y, Amano T, Matsubayashi H, et al. Effect of antiepileptic drugs on absence-like seizures in the tremor rat. Epilepsia 1995;36:938–42.
[18] Marescaux C, Micheletti G, Vergnes M, Depaulis A, Rumbach L, Warter JM. A model of chronic spontaneous petit mal-like seizures in the rat: comparison with pentylenetetrazol-induced seizures. Epilepsia 1984;25:326–31.
[19] van Rijn CM, Sun MS, Deckers CL, Edelbroek PM, Keyser A, Renier W, et al. Effects of the combination of valproate and ethosuximide on spike wave discharges in WAG/Rij rats. Epilepsy Res 2004;59:181–9.
[20] Kobayashi K, Nishibayashi N, Ohtsuka Y, Oka E, Ohtahara S. Epilepsy with electrical status epilepticus during slow sleep and secondary bilateral synchrony. Epilepsia 1994;35:1097–103.
[21] Tassinari CA, Rubboli G, Volpi L, Meletti S, D'Orsi G, Franca M, et al. Encephalopathy with electrical status epilepticus during slow sleep or ESES syndrome including the acquired aphasia. Clinical Neurophysiol 2000;111(Suppl. 2):S94–S102.
[22] Patry G, Lyagoubi S, Tassinari CA. Subclinical "electrical status epilepticus" induced by sleep in children. A clinical and electroencephalographic study of six cases. Arch Neurol 1971;24:242–52.

ELSEVIER

Brain & Development 37 (2015) 515–526

BRAIN & DEVELOPMENT
Official Journal of the Japanese Society of Child Neurology

www.elsevier.com/locate/braindev

Original article

Microarray analysis of 50 patients reveals the critical chromosomal regions responsible for 1p36 deletion syndrome-related complications

Shino Shimada [a,b], Keiko Shimojima [a], Nobuhiko Okamoto [c], Noriko Sangu [a,d], Kyoko Hirasawa [b], Mari Matsuo [e], Mayo Ikeuchi [f], Shuichi Shimakawa [g], Kenji Shimizu [h], Seiji Mizuno [i], Masaya Kubota [j], Masao Adachi [k], Yoshiaki Saito [l], Kiyotaka Tomiwa [m], Kazuhiro Haginoya [n], Hironao Numabe [o], Yuko Kako [p], Ai Hayashi [q], Haruko Sakamoto [r], Yoko Hiraki [s], Koichi Minami [t], Kiyoshi Takemoto [u], Kyoko Watanabe [v], Kiyokuni Miura [w], Tomohiro Chiyonobu [x], Tomohiro Kumada [y], Katsumi Imai [z], Yoshihiro Maegaki [aa], Satoru Nagata [b], Kenjiro Kosaki [ab], Tatsuro Izumi [f], Toshiro Nagai [ac], Toshiyuki Yamamoto [a,*]

[a] *Tokyo Women's Medical University Institute for Integrated Medical Sciences, Tokyo, Japan*
[b] *Department of Pediatrics, Tokyo Women's Medical University, Tokyo, Japan*
[c] *Department of Medical Genetics, Osaka Medical Center and Research Institute for Maternal and Child Health, Izumi, Japan*
[d] *Department of Oral and Maxillofacial Surgery, School of Medicine, Tokyo Women's Medical University, Tokyo, Japan*
[e] *Institute of Medical Genetics, Tokyo Women's Medical University, Tokyo, Japan*
[f] *Department of Pediatrics and Child Neurology, Oita University Faculty of Medicine, Oita, Japan*
[g] *Department of Pediatrics, Osaka Medical College, Takatsuki, Japan*
[h] *Division of Medical Genetics, Saitama Children's Medical Center, Saitama, Japan*
[i] *Department of Pediatrics, Central Hospital, Aichi Human Service Center, Kasugai, Japan*
[j] *Division of Neurology, National Center for Child Health and Development, Tokyo, Japan*
[k] *Department of Pediatrics, Kakogawa Hospital Organization, Kakogawa West-City Hospital, Kakogawa, Japan*
[l] *Department of Child Neurology, National Center of Neurology and Psychiatry, Tokyo, Japan*
[m] *Department of Pediatrics, Medical Center for Children, Osaka City General Hospital, Osaka, Japan*
[n] *Department of Pediatric Neurology, Takuto Rehabilitation Center for Children, Sendai, Japan*
[o] *Department of Genetic Counseling, Graduate School of Humanities and Sciences, Ochanomizu University, Tokyo, Japan*
[p] *Department of Pediatrics, Showa University School of Medicine, Tokyo, Japan*
[q] *Department of Neonatology, Japanese Red Cross Kyoto Daiichi Hospital, Kyoto, Japan*
[r] *Department of Pediatrics, Osaka Red Cross Hospital, Osaka, Japan*
[s] *Hiroshima Municipal Center for Child Health and Development, Hiroshima, Japan*
[t] *Department of Pediatrics, Wakayama Medical University, Wakayama, Japan*
[u] *Osaka Developmental Rehabilitation Center, Osaka, Japan*
[v] *Department of Pediatrics, National Hospital Organization Kokura Medical Center, Kitakyushu, Japan*
[w] *Developmental Disability Medicine, Nagoya University Graduate School of Medicine, Nagoya, Japan*
[x] *Department of Pediatrics, Graduate School of Medical Science, Kyoto Prefectural University of Medicine, Kyoto, Japan*
[y] *Department of Pediatrics, Shiga Medical Center for Children, Moriyama, Japan*
[z] *National Epilepsy Center, Shizuoka Institute of Epilepsy and Neurological Disorders, Shizuoka, Japan*

* Corresponding author. Address: Tokyo Women's Medical University Institute for Integrated Medical Sciences, 8-1 Kawada-cho, Shinjuku-ward, Tokyo 162-8666, Japan. Tel.: +81 3 3353 8111x24013; fax: +81 3 5269 7667.
E-mail address: yamamoto.toshiyuki@twmu.ac.jp (T. Yamamoto).

http://dx.doi.org/10.1016/j.braindev.2014.08.002

[aa] Division of Child Neurology, Tottori University School of Medicine, Yonago, Japan
[ab] Center for Medical Genetics, Keio University School of Medicine, Tokyo, Japan
[ac] Department of Pediatrics, Dokkyo Medical University Koshigaya Hospital, Saitama, Japan

Received 2 April 2014; received in revised form 1 August 2014; accepted 5 August 2014

Abstract

Objective: Monosomy 1p36 syndrome is the most commonly observed subtelomeric deletion syndrome. Patients with this syndrome typically have common clinical features, such as intellectual disability, epilepsy, and characteristic craniofacial features.

Method: In cooperation with academic societies, we analyzed the genomic copy number aberrations using chromosomal microarray testing. Finally, the genotype–phenotype correlation among them was examined.

Results: We obtained clinical information of 86 patients who had been diagnosed with chromosomal deletions in the 1p36 region. Among them, blood samples were obtained from 50 patients (15 males and 35 females). The precise deletion regions were successfully genotyped. There were variable deletion patterns: pure terminal deletions in 38 patients (76%), including three cases of mosaicism; unbalanced translocations in seven (14%); and interstitial deletions in five (10%). Craniofacial/skeletal features, neurodevelopmental impairments, and cardiac anomalies were commonly observed in patients, with correlation to deletion sizes.

Conclusion: The genotype–phenotype correlation analysis narrowed the region responsible for distinctive craniofacial features and intellectual disability into 1.8–2.1 and 1.8–2.2 Mb region, respectively. Patients with deletions larger than 6.2 Mb showed no ambulation, indicating that severe neurodevelopmental prognosis may be modified by haploinsufficiencies of *KCNAB2* and *CHD5*, located at 6.2 Mb away from the telomere. Although the genotype–phenotype correlation for the cardiac abnormalities is unclear, *PRDM16*, *PRKCZ*, and *RERE* may be related to this complication. Our study also revealed that female patients who acquired ambulatory ability were likely to be at risk for obesity.

Keywords: 1p36 deletion syndrome; Chromosomal deletion; Genotype–phenotype correlation; Intellectual disability; Ambulation; Epilepsy; Distinctive features

1. Introduction

Monosomy 1p36 syndrome is a congenital malformation syndrome caused by the subtelomeric deletion of the short arm of chromosome 1 [1–3]. This syndrome is the most commonly observed subtelomere deletion syndrome, with an estimated incidence of 1:5000–1:10,000 [4,5]. Patients with this syndrome exhibit common clinical features, including intellectual disability (ID) and characteristic craniofacial features; such as straight eyebrows, deep-set eyes, epicanthus, and a pointed chin [6–9]. Although the levels of ID vary among patients, craniofacial features are commonly seen [10]. The patients with the 1p36 deletion syndrome also show many other complications, including hypotonia, seizures, hearing loss, structural heart defects, cardiomyopathy, ophthalmological abnormalities, and behavior abnormalities [7]. Recent advances in microarray-based chromosomal testing have helped us to identify small chromosomal rearrangements that are invisible by conventional G-banded chromosomal tests/karyotyping [11,12]. Using this method, the precise locations of the aberrations can be revealed at the molecular level. These advances have also allowed the study of more in-depth genotype–phenotype correlations for this syndrome, as well as the identification of some of the regions responsible for individual complications [12,13].

In this study, we performed a nation-wide survey for the 1p36 deletion syndrome in Japan. The aim of this study was to identify the chromosomal regions responsible for individual complications in patients with 1p36 deletions. We analyzed the affected genomic regions in 50 patients with 1p36 deletions, and performed correlational analyses of the genotype data with the clinical information.

2. Materials and methods

2.1. Patients and samples

We performed a nation-wide survey for the 1p36 deletion syndrome with the cooperation of two academic societies; the Japanese Society of Child Neurology and the Japan Society of Pediatric Genetics. The study subjects were Japanese patients who had already been diagnosed using various diagnostic methods, including conventional karyotyping, subtelomere fluorescence *in situ* hybridization (FISH) analysis, multiplex ligation-dependent probe amplification (MLPA), and chromosomal microarray testing. Five patients